

A superradiant black hole rocket

Lucas Acito,^{*} Nicolás E. Grandi,[†] and Pablo Pisani[‡]

Instituto de Física La Plata - CONICET & Departamento de Física UNLP,

C.C. 67, 1900 La Plata, Argentina

We calculate the total thrust resulting from the interaction between charged scalar modes and a superradiant Reissner-Nordström black hole, when the modes are deflected by a hemispherical perfect mirror located at a finite distance from the black hole's horizon.

I. INTRODUCTION

The superradiance phenomenon in black hole physics refers to the emergence of a particle from a scattering process with more energy than that of the incident state. This implies that energy can be extracted from a black hole.

However, the above description raises two important questions. Firstly, what happens to the one-way nature of the black hole horizon? The answer is that energy is extracted from the black hole in plane wave states that do not contain information. Secondly, as energy is taken from the black hole, how do we ensure that its entropy doesn't decrease? The answer lies in the fact that superradiance only occurs when there is a second charge which allows the horizon area to increase as the energy is removed [1].

Initially, superradiance was described in the context of Kerr black holes, where angular momentum serves as the second charge [2]. However, it can also be observed in electrically charged Reissner-Nordström black holes [3]. The advantage here is that these black holes are spherically symmetric, making the analysis of wave modes around them simpler.

The purpose of this note is to investigate whether the superradiant effect can be harnessed to extract momentum from a black hole and generate thrust.

^{*} lucasacito@gmail.com

[†] grandi@fisica.unlp.edu.ar

[‡] pisani@fisica.unlp.edu.ar

II. THE SETUP

The idea we want to test is whether the superradiant phenomenon, which allows to extract energy from a black hole, can be also used to extract momentum. To keep the calculations as simple as possible, we concentrate in a spherically symmetric charged black hole. In contact with a thermal bath, the black hole superradiates low energy charged particles until equilibrium is reached. To collect the momentum, we use a semi-spherical mirror centered at the black hole, as shown in Fig. 1.

To make this proposal concrete, we set a Reissner-Nordström black hole in asymptotically flat space as a background solution. The bath is made of probe plane wave modes of a charged massive scalar field, featuring a thermal energy distribution at finite chemical potential. The scalar modes are scattered by the black hole and reflected at the mirror, ultimately leading to the total thrust that we aim to compute.

In order to do that, we first solve the classical scattering problem of a scalar plane wave hitting the black hole and mirror system. Then, putting the scalar on a thermal atmosphere corresponds to averaging on the plane wave directions isotropically, and on its energy with a thermal Bose-Einstein distribution.

The total thrust can be then calculated as the flux of the scalar energy momentum tensor on a sphere centered at the black-hole and enclosing the mirror.

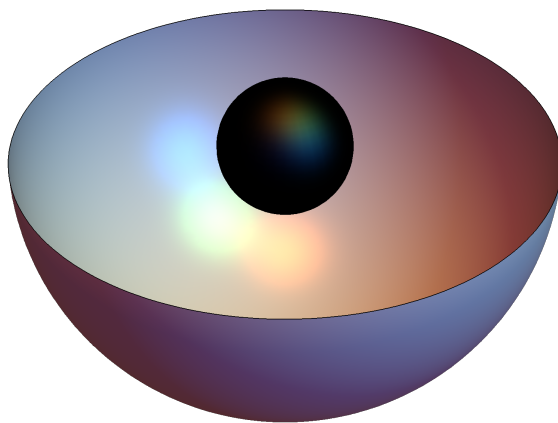


FIG. 1: A hemispherical perfect mirror around a Reissner-Nordström black hole.

III. SCALAR MODES ON A REISSNER-NORDSTRÖM BLACK HOLE

Reissner-Nordström black holes are charged solutions to the Einstein-Maxwell field equations, which have a metric and an electromagnetic field with the form [4]

$$ds^2 = -f dt^2 + \frac{1}{f} dr^2 + r^2 d\Omega_2^2 \quad A = h dt \quad (1)$$

here the lapse $f(r)$ and the electrostatic potential $h(r)$ are functions of r given by

$$f = 1 - \frac{2M}{r} + \frac{Q^2}{r^2} \quad h = -\frac{Q}{r} + \mu \quad (2)$$

The integration constants M and Q correspond to the ADM mass and charge respectively. Non-extremal solutions $M > Q$ generically have two horizons that we denote $r = r_{\pm}$.

The equation for a charged Klein-Gordon field with charge e and mass m in the above background reads

$$\frac{1}{r^2} \partial_r (r^2 f \partial_r \Phi) + \left(\frac{1}{r^2} \nabla_{\Omega}^2 - \frac{(\partial_t - ieh)^2}{f} - m^2 \right) \Phi = 0 \quad (3)$$

where ∇_{Ω}^2 is the Laplace operator on the two-sphere, with eigenvalues $-\ell(\ell+1)$ and eigenfunctions given by the spherical harmonics $Y_{\ell}^m(\theta, \phi) = \sqrt{(2\ell+1)/4\pi} \sqrt{(\ell-m)!/(\ell+m)!} e^{im\phi} P_{\ell}^m(\cos\theta)$ where P_{ℓ}^m is the associated Legendre polynomial. If we consider a solution with energy ω we can decompose the scalar field as

$$\Phi(r, \theta, \phi, t) = e^{-i\omega t} \sum_{\ell, m} \alpha_{\ell}^m R_{\ell}(r) Y_{\ell}^m(\theta, \phi) \quad (4)$$

Where α_{ℓ}^m are coefficients that depends on ω which are determined once the boundary conditions are imposed. Plugging back into the equations of motion, we get an equation for the radial dependence in the form

$$\frac{1}{r^2} \partial_r (r^2 f \partial_r R_{\ell}) + \left(\frac{(\omega + eh)^2}{f} - \frac{\ell(\ell+1)}{r^2} - m^2 \right) R_{\ell} = 0 \quad (5)$$

Notice that the equation is independent of the spherical index m , which was anticipated in (4) when we omitted to include it as a label for R_{ℓ} .

We solve the above equation imposing causal (in-going) boundary conditions at the outer horizon r_+ . At infinity, we impose the conditions of a scattering problem: an incident Coulomb wave with energy ω and propagating in an arbitrary direction \tilde{n} , added to the corresponding scattered outgoing spherical wave. The inner and outer solutions are matched at a finite radius $r_0 > r_+$, where we place a perfect mirror in the southern hemisphere (Fig 1) at which the scalar field vanishes.

A. Boundary conditions at the horizon

Close to the outer black hole horizon $r = r_+$, the lapse function can be expanded as $f(r) = 4\pi T_{BH} (r - r_+)$ where $T_{BH} = f'(r_+)/4\pi$ is the Hawking temperature [5]. The radial equation is then approximated by

$$\partial_{\log(r-r_+)}^2 R_\ell + \left(\frac{\omega - \omega_s}{4\pi T_{BH}} \right)^2 R_\ell \simeq 0 \quad (6)$$

where we defined the superradiant frequency ω_s as $\omega_s = e(\mu_{BH} - \mu)$ with $\mu_{BH} = Q/r_+$. Equation (6) has two linearly independent solutions representing in-going and out-going waves. We call $u_\ell(r)$ the solution to the full radial equation (5) that close to the black hole horizon behaves as an in-going wave

$$u_\ell(r) \simeq e^{i\kappa \log(r-r_+)} \quad \text{with} \quad \kappa = -\frac{\omega - \omega_s}{4\pi T_{BH}} \quad (7)$$

This represents a plane wave with group velocity $v_g = \partial\omega/\partial\kappa = -4\pi T_{BH}$. Since $v_g < 0$ then wave packets (*i.e.* information) are falling into the black hole horizon. On the other hand the phase velocity is $v_f = \omega/\kappa = -4\pi T_{BH}\omega/(\omega - \omega_s)$. Then, if $\omega < \omega_s$ we have $v_f > 0$ and plane waves (*i.e.* energy) are being radiated from the horizon. This condition characterizes a superradiant mode.

Notice that the superradiant behavior takes place as long as $\omega_s \neq 0$ or in other words $\mu \neq \mu_{BH}$. This can be interpreted as the black hole not being at equilibrium with its environment. Indeed, since $A(r_+) = \mu - \mu_{BH}$, the gauge field does not vanish at the horizon, which would imply a conical singularity in the corresponding Euclidean continuation.

Imposing in-going boundary conditions at the horizon entails writing the solution in the form (4) in the region between the horizon and the mirror, choosing the in-going form for the radial part $R_\ell(r) = u_\ell(r)$,

$$\Phi^-(r, \vartheta, \varphi, t) = e^{-i\omega t} \sum_{\ell, m} a_\ell^m \frac{u_\ell(r)}{u_\ell(r_0)} Y_\ell^m(\theta, \phi), \quad r_+ < r < r_0. \quad (8)$$

Here we rescaled the coefficient as $\alpha_\ell^m = a_\ell^m/u_\ell(r_0)$ in order to simplify the forthcoming calculations.

B. Boundary conditions at infinity

When the radial coordinate goes to infinity, we can expand the radial equation (5) as

$$\frac{1}{r^2} \partial_r (r^2 \partial_r R_\ell(r)) + \left(k^2 - \frac{2\eta}{r} - \frac{\ell(\ell+1) + \dots}{r^2} \right) R_\ell(r) = 0 \quad (9)$$

with $k^2 = (\omega + e\mu)^2 - m^2$ and $\eta = Q(\omega + e\mu) - 2Mk^2 - Mm^2$. This corresponds to a Coulomb scattering problem, with solutions behaving as out-going spherical waves [6]. Calling $(-i)^{\ell+1} v_\ell(r)$ to the solution to the full radial equation (5) that matches such behavior at infinity, we have

$$v_\ell(r) \simeq \frac{1}{(kr)^{1+i\eta}} e^{ikr} \quad (10)$$

The scattered part of the scalar field can then be written as in (4) with the radial solution replaced by its out-going form $R_\ell(r) = v_\ell(r)$,

$$\Phi^{\text{scat}}(r, \theta, \phi, t) = e^{-i\omega t} \sum_{\ell, m} b_\ell^m \frac{v_\ell(r)}{v_\ell(r_0)} Y_\ell^m(\theta, \phi), \quad r > r_0, \quad (11)$$

where again we have rescaled $\alpha_\ell^m = b_\ell^m / v_\ell(r_0)$ for future use.

Regarding the incident wave, we consider a plane wave with momentum $\vec{k} = k \check{n}$, with $\omega_\pm = \pm \sqrt{k^2 + m^2} - e\mu$, and amplitude $A_{\vec{k}}^\pm$, which in the Coulomb background picks a power law factor. It can be decomposed in out-going and in-going spherical waves as

$$\begin{aligned} \Phi^{\text{inc}}(r, \theta, \phi, t) &= \frac{\mathcal{N}_\pm}{4\pi} A_{\vec{k}}^\pm e^{i(kr \check{n} \cdot \check{r} - \omega_\pm t)} (kr)^{-i\eta} (1 - \check{n} \cdot \check{r})^{-i\eta} \\ &\simeq -i \mathcal{N}_\pm A_{\vec{k}}^\pm \sum_{\ell m} Y_\ell^{m*}(\check{n}) Y_\ell^m(\theta, \phi) \left(\frac{e^{ikr}}{(2kr)^{1+i\eta}} - (-1)^\ell \frac{e^{-ikr}}{(2kr)^{1-i\eta}} \right) e^{-i\omega_\pm t}. \end{aligned} \quad (12)$$

Now, calling $i^{\ell+1} w_\ell(r)$ to the solution that behaves as the parenthesis at infinity, we can write the incident part of the scalar field as

$$\Phi^{\text{inc}}(r, \theta, \phi, t) = e^{-i\omega_\pm t} \sum_{\ell, m} c_\ell^m \frac{w_\ell(r)}{w_\ell(r_0)} Y_\ell^m(\theta, \phi), \quad r > r_0, \quad (13)$$

with $c_\ell^m = i^\ell \mathcal{N}_\pm A_{\vec{k}}^\pm Y_\ell^{m*}(\check{n}) w_\ell(r_0)$. Notice that at infinity we have $w_\ell(r) \propto \Re\{v_\ell(r)\}$ and since both $w_\ell(r)$, $v_\ell(r)$ solve the same linear equation, then this relation holds for all r .

The outer solution is a superposition of the incident and the scattered parts. In consequence, for $r > r_0$ the solution reads

$$\begin{aligned} \Phi^+(r, \theta, \phi, t) &= \Phi^{\text{inc}}(r, \theta, \phi, t) + \Phi^{\text{scat}}(r, \theta, \phi, t) \\ &= e^{-i\omega_\pm t} \sum_{\ell, m} \left(b_\ell^m \frac{v_\ell(r)}{v_\ell(r_0)} + c_\ell^m \frac{w_\ell(r)}{w_\ell(r_0)} \right) Y_\ell^m(\theta, \phi), \quad r > r_0. \end{aligned} \quad (14)$$

C. Matching at the mirror

The mirror is a hemispherical shell centered at the black hole that sits at a fixed radius at the southern hemisphere. For a perfect mirror the scalar field vanishes at its surface. We then impose that the scalar field must be zero at $r = r_0$ for $\frac{\pi}{2} \leq \theta \leq \pi$,

$$\Phi(r_0, \theta, \phi, t) = 0 \quad \frac{\pi}{2} \leq \theta \leq \pi. \quad (15)$$

On the other hand, the wave function is continuous on the sphere $r = r_0$,

$$\Phi^+(r_0, \theta, \phi, t) = \Phi^-(r_0, \theta, \phi, t) \quad 0 \leq \theta \leq \pi, \quad (16)$$

whereas the radial derivative is continuous only on the northern hemisphere

$$\frac{d}{dr}\Phi^+(r, \theta, \phi, t)|_{r=r_0} = \frac{d}{dr}\Phi^-(r, \theta, \phi, t)|_{r=r_0} \quad 0 \leq \theta \leq \frac{\pi}{2}. \quad (17)$$

These three matching conditions at $r = r_0$ determine the coefficients a_ℓ^m and b_ℓ^m in (8) and (11) in terms of c_ℓ^m in (13) or, equivalently, the incident amplitudes A_k^\pm . In particular, continuity of the wave function at $r = r_0$ implies

$$b_\ell^m = a_\ell^m - c_\ell^m \quad (18)$$

so we just have to determine the coefficients a_ℓ^m . Since the solution vanishes at the mirror, we have

$$0 = \sum_{\ell m} a_\ell^m Y_\ell^m(\theta, \phi) \quad \text{for } \frac{\pi}{2} \leq \theta \leq \pi. \quad (19)$$

On the other hand, continuity of the radial derivative at $r = r_0$ implies

$$0 = \sum_{\ell, m} (\mathcal{H}_\ell a_\ell^m - \mathcal{I}_\ell c_\ell^m) Y_\ell^m(\theta, \phi) \quad \text{for } 0 \leq \theta \leq \frac{\pi}{2}, \quad (20)$$

where

$$\mathcal{H}_\ell = \frac{u'_\ell(r_0)}{u_\ell(r_0)} - \frac{v'_\ell(r_0)}{v_\ell(r_0)}, \quad \mathcal{I}_\ell = \frac{w'_\ell(r_0)}{w_\ell(r_0)} - \frac{v'_\ell(r_0)}{v_\ell(r_0)} = -\frac{i}{kr_0^2 f(r_0)} \frac{1}{w_\ell(r_0)v_\ell(r_0)}. \quad (21)$$

In the second equality we use the Wronskian definition and the asymptotic value of the functions. Expressions (19) and (20) hold for any $\phi \in (0, 2\pi)$ so they immediately lead to

$$0 = \sum_{\ell=|m|}^{\infty} (-1)^\ell a_\ell^m \sqrt{(2\ell+1)} \sqrt{\frac{(\ell-m)!}{(\ell+m)!}} P_\ell^m(x), \quad (22)$$

$$0 = \sum_{\ell=|m|}^{\infty} (\mathcal{H}_\ell a_\ell^m - \mathcal{I}_\ell c_\ell^m) \sqrt{(2\ell+1)} \sqrt{\frac{(\ell-m)!}{(\ell+m)!}} P_\ell^m(x), \quad (23)$$

for each $m \in \mathbb{Z}$ and $0 \leq x = \cos \theta \leq 1$. Using that the associated Legendre polynomials $P_\ell^m(x)$ and $P_{\ell'}^m(x)$ are orthogonal in the interval $(0, 1)$ whenever $\ell - \ell'$ is even, we obtain

$$0 = a_\ell^m - \sum_{\ell' \geq |m|} (\gamma_{\ell\ell'}^m - \delta_{\ell\ell'}) a_{\ell'}^m, \quad (24)$$

$$0 = \mathcal{H}_\ell a_\ell^m - \mathcal{I}_\ell c_\ell^m + \sum_{\ell' \geq |m|} (\gamma_{\ell\ell'}^m - \delta_{\ell\ell'}) (\mathcal{H}_{\ell'} a_{\ell'}^m - \mathcal{I}_{\ell'} c_{\ell'}^m), \quad (25)$$

where we have introduced the coefficients

$$\gamma_{\ell\ell'}^m = \sqrt{\frac{(2\ell+1)(2\ell'+1)(\ell-m)!(\ell'-m)!}{(\ell+m)!(\ell'+m)!}} \times \int_0^1 dx P_\ell^m(x) P_{\ell'}^m(x), \quad (26)$$

which take the particular values $\gamma_{\ell\ell'}^m = 0$ for $\ell - \ell'$ even and $\gamma_{\ell\ell}^m = 1$. Note that with this values the only non zero components in the sums (24) and (25) are with $\ell - \ell'$ odd, but the used notation is more convenient. The matrix γ^m of coefficients $\gamma_{\ell\ell'}^m$ is real and symmetric and it satisfies $(\gamma^m)^2 = 2\gamma^m$ and $(\gamma^m - \mathbf{1})^{-1} = \gamma^m - \mathbf{1}$ (where $\mathbf{1}$ is the identity matrix). The set of matrices γ^m is even in the index m satisfying $\gamma^{-m} = \gamma^m$.

Replacing expression (24) in (25) and regrouping the coefficients, the result reads

$$\sum_{h=|m|}^{\infty} M_{\ell h}^m a_h^m = \sum_{\ell'=|m|}^{\infty} c_{\ell'}^m \mathcal{I}_{\ell'} \gamma_{\ell\ell'}^m, \quad (27)$$

valid for any $\ell \geq |m|$ and where

$$(M_m)_{\ell h} = [-\mathcal{H}(\gamma^m - \mathbf{1}) - (\gamma^m - \mathbf{1})\mathcal{H} + \gamma^m \mathcal{H} \gamma^m]_{\ell h} \quad (28)$$

with \mathcal{H} a diagonal matrix of elements \mathcal{H}_ℓ . As a consequence, we finally have

$$a_\ell^m = \sum_{\ell'=|m|}^{\infty} (O_{\ell\ell'}^m + \delta_{\ell\ell'}) c_{\ell'}^m, \quad b_\ell^m = \sum_{\ell'=|m|}^{\infty} O_{\ell\ell'}^m c_{\ell'}^m, \quad (29)$$

where

$$O_{\ell\ell'}^m = -\frac{i}{k r_0^2 f(r_0)} \frac{1}{w_{\ell'}(r_0) v_{\ell'}(r_0)} [M_m^{-1} \gamma^m]_{\ell\ell'} - \delta_{\ell\ell'} \quad (30)$$

With this, we get the coefficients a_ℓ and b_ℓ in terms of the functions $u_\ell(r)$, $v_\ell(r)$ and $w_\ell(r)$, which have to be obtained numerically by solving the radial equation (5) with the appropriate boundary conditions (7), (10) and (12) respectively, and the matrix elements $\gamma_{\ell\ell'}^m$ of (26).

D. Numerical Analysis

In this section we analyse the classical field obtained from the previous sections that fulfill all the boundary conditions. To do so, we need to obtain numerically the radial solutions $u_\ell(r)$, $v_\ell(r)$ and $w_\ell(r)$ of the radial equation (5), and compute $\gamma_{\ell\ell}^m$. These components characterize the field obtained in the whole space, in terms of the incident wave amplitude A_k^\pm and direction \tilde{n} which are free parameters.

In order to obtain numerically $u_\ell(r)$ that satisfies the near horizon behavior (7), first we extend the in-going wave to a finite radius away from the horizon to avoid the singularity, and then solve numerically up to the mirror. On the other hand, $v_\ell(r)$ and $w_\ell(r)$ are obtained numerically by shooting, integrating from some arbitrary initial condition at the mirror up to a distance where the space-curvature effect is negligible; and there fitting with the asymptotic behavior (10) and (12). For further details, see the open code [7]. Lastly, the matrix of coefficients $\gamma_{\ell\ell}^m$ are numerical integrals which can be seen in Appendix B 1.

To gain some intuition on the resulting field, we first consider the flat space case (see Fig. 2, first line) with an isotropic set of incoming waves with equal fixed amplitude A_k^\pm . In this case, the radial solutions are the spherical Bessel functions $(-i)^{\ell+1}u_\ell(r) = (-i)^{\ell+1}w_\ell(r) = j_\ell(kr)$ and the first kind spherical Hankel functions $(-i)^{\ell+1}v_\ell(r) = h_\ell^{(1)}(kr)$. On the left plot we see the charge density $|\Phi^2|$ on a plane that contains the z axis. We can see the spherical aberration pattern in the form of a high intensity vertical region at the center of the plot, as expected for a hemispherical mirror. The field Φ as a function of the variable z is depicted on the right, where we can see how the matching works at the mirror radius. We can expect that, as particles are coming from every direction, the mirror would move downwards, since there are more particles impinging from the concave side of the mirror. As a consequence, we have a ‘background force’ acting on the mirror.

Next we consider the charged black hole background in the second and third lines of figure 2. There, we show two different energies, the plots on the second line correspond to the non-superradiant regime $\omega > \omega_s$, while those on the third have superradiant energies $\omega < \omega_s$. Again, we can see how the matching of the field works in the z direction and also the behavior near the black hole. On the left we can see clearly how the black hole rocket works, as the energy going out from the black hole due to superradiance pushes on the mirror.

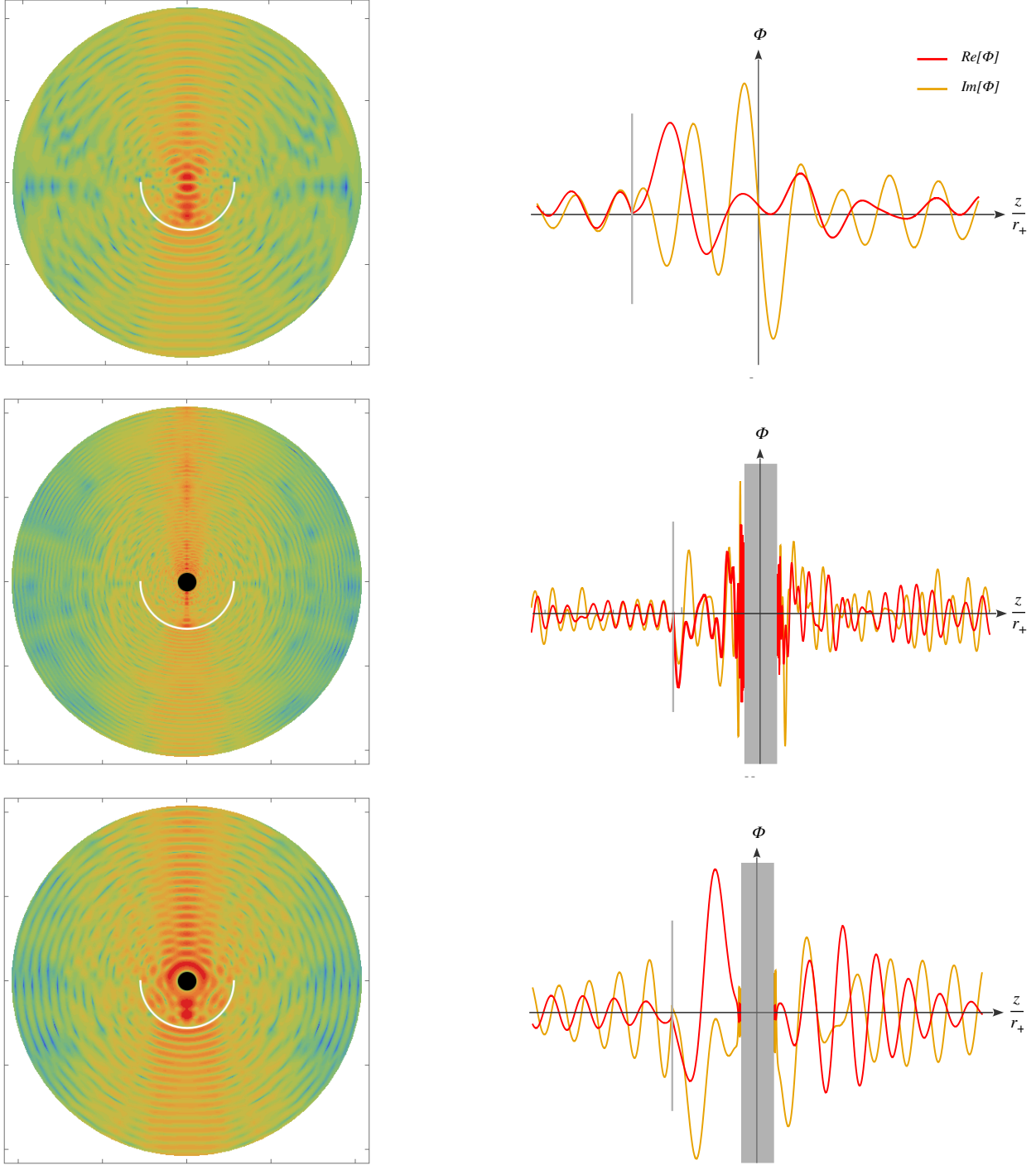


FIG. 2: Classical field for a superposition of incident waves with $0 \leq \theta \leq \pi$ with $m = 0.1$ and $e = 0.5$. Left: Amplitude $|\Phi|^2$ on a transverse plane containing the z axis. Right: Field $\Phi(0,0,z)$ as a function of z . First line: on flat space $M = Q = 0$ with $k = 0.3$. Second and third lines: on a black hole with $M = 9.9$, $Q = 0.99$, with $k = 0.6$ (non-superradiant mode) and $k = 0.3$ (superradiant mode) respectively.

IV. CALCULATION OF THE THRUST

A. Quantization

In the previous sections we have written the full solution for a classical scalar field corresponding to an incident plane wave that scatters at the hemispherical mirror and satisfies in-going conditions at the black hole horizon. Next, we will submerge the setting in a bath of charged scalar particles [8] at temperature T and chemical potential μ . In order to satisfy the canonical relation $[\Phi(t, \vec{x}), \dot{\Phi}^\dagger(t, \vec{y})] = i\delta^{(3)}(\vec{x} - \vec{y})$, we chose the normalization

$$\mathcal{N}_\pm = \frac{|\omega_\pm + \mathbf{e}\mu|}{2\pi^2 \sqrt{|\omega_+ \omega_-|}} \frac{1}{\sqrt{\pm 2\omega_\pm}} \quad (31)$$

In this way, the operators $\hat{A}_{\vec{k}}^\dagger$ and $\hat{B}_{\vec{k}}^\dagger$, which are the quantum upgrade of the amplitudes $A_{\vec{k}}^+$ and $A_{\vec{k}}^-$ of the classical field (12), create particles and anti-particles with momentum \vec{k} and satisfy the usual algebra $[\hat{A}_{\vec{k}}, \hat{A}_{\vec{k}'}^\dagger] = [\hat{B}_{\vec{k}}, \hat{B}_{\vec{k}'}^\dagger] = (2\pi)^3 \delta(\vec{k} - \vec{k}')$.

Now we assume an isotropic thermal distribution of plane waves with temperature T and chemical potential μ . This implies that the expectation values of the quadratic operators $\hat{A}_{\vec{k}}^\dagger \hat{A}_{\vec{k}'}$ and $\hat{B}_{\vec{k}}^\dagger \hat{B}_{\vec{k}'}$ are given by the thermal Bose-Einstein distribution, in the form [9]

$$\langle \hat{A}_{\vec{k}}^\dagger \hat{A}_{\vec{k}'} \rangle = \frac{1}{e^{\frac{\omega_+}{T}} - 1} (2\pi)^3 \delta^3(\vec{k} - \vec{k}'), \quad \langle \hat{B}_{\vec{k}}^\dagger \hat{B}_{\vec{k}'} \rangle = \frac{1}{e^{-\frac{\omega_-}{T}} - 1} (2\pi)^3 \delta^3(\vec{k} - \vec{k}'). \quad (32)$$

Any other expectation value quadratic in those operators is zero.

B. Total thrust

To calculate the thrust induced on the system by the field modes, we use the energy momentum tensor of the scalar field. The flux of any of its spatial components through a spherical surface enclosing the system at infinity gives the total force in the corresponding direction.

$$F_j = \int_{r \rightarrow \infty} d\Omega_2 n_r^i T_{ij} = \int_{r \rightarrow \infty} d\Omega_2 (\partial_j r T_{rr} + \partial_j \theta T_{r\theta} + \partial_j \varphi T_{r\varphi}) , \quad (33)$$

where the indices i, j refer to the asymptotic Cartesian coordinates x^i , and the unit vector n_r^i points in the radial direction.

In the first term in (33) we have $\partial_i r = x^i/r = (\cos \varphi \sin \theta, \sin \varphi \sin \theta, \cos \theta)$. Due to the symmetry of the setting, the energy momentum tensor at spatial infinity does not depend on φ so the only non-vanishing component of the thrust from the first term in the integrand points in the z direction. Regarding the second term, we have $r\partial_i\theta = (\cos \varphi \cos \theta, \sin \varphi \cos \theta, -\sin \theta)$, so again only the z component remains. For similar reasons, there is no contribution from the third term. We are left with

$$F_j = \delta_{jz} 2\pi \int_0^\pi d\theta \sin \theta (\cos \theta r^2 T_{rr} - \sin \theta r T_{r\theta}) \Big|_{r \rightarrow \infty} \quad (34)$$

We use the energy momentum tensor obtained as the mean value of the corresponding quantum expression (see Appendix A). The needed components T_{rr} and $T_{r\theta}$ at $r \rightarrow \infty$ are

$$T_{rr} = \frac{1}{2} (\partial'_t \partial_t + i\mathbf{e}\mu(\partial'_t - \partial_t) + \partial_r \partial'_r - m^2 + \mathbf{e}^2 \mu^2) \langle : \hat{\Phi}^\dagger(\mathbf{x}) \hat{\Phi}(\mathbf{x}') : \rangle \Big|_{\mathbf{x}'=\mathbf{x}} \quad (35)$$

$$T_{r\theta} = \frac{1}{2} (\partial_r \partial'_\theta + \partial'_r \partial_\theta) \langle : \hat{\Phi}^\dagger(\mathbf{x}) \hat{\Phi}(\mathbf{x}') : \rangle \Big|_{\mathbf{x}'=\mathbf{x}} \quad (36)$$

with the colons $:\cdot:$ denoting normal ordering. Here $rT_{r\theta}$ vanishes at infinity and for $r^2 T_{rr}$ we have (see Appendix A)

$$r^2 T_{rr} = \int_0^\infty dk \frac{|\omega_+ + \mathbf{e}\mu|^2 k^2}{\pi |\omega_+ \omega_-|} \left(\frac{1}{\omega_+ (e^{\frac{\omega_+}{T}} - 1)} - \frac{1}{\omega_- (e^{-\frac{\omega_-}{T}} - 1)} \right) \sum_{\ell, \ell', m} \mathcal{U}_{\ell\ell'} Y_\ell^{m*}(\theta, \phi) Y_{\ell'}^m(\theta, \phi) \quad (37)$$

where we defined

$$\mathcal{U}_{\ell\ell'}^m = \sum_{\ell''=|m|} e^{i\frac{\pi}{2}(\ell-\ell')} \frac{|w_{\ell''}(r_0)|^2}{v_\ell^*(r_0) v_{\ell'}(r_0)} O_{\ell\ell''}^{m*} O_{\ell'\ell''}^m + \Re \left[e^{i\frac{\pi}{2}(\ell-\ell')} \frac{w_\ell(r_0)}{v_{\ell'}(r_0)} O_{\ell\ell'}^m \right] \quad (38)$$

Inserting into (33) and computing the angular integral, we get

$$F_z = \frac{1}{\pi r_0^2 f(r_0)} \int_0^\infty dk \frac{|\omega_+ + \mathbf{e}\mu|^2 k^2}{\pi |\omega_+ \omega_-|} \left(\frac{1}{\omega_+ (e^{\frac{\omega_+}{T}} - 1)} - \frac{1}{\omega_- (e^{-\frac{\omega_-}{T}} - 1)} \right) \times \\ \times \sum_m \sum_{\ell=|m|} \sqrt{\frac{(\ell-m)(\ell+m)}{(2\ell+1)(2\ell-1)}} \Re \left[\frac{1}{v_{\ell-1}^*(r_0) v_\ell(r_0)} \left([M_m^{-1} \gamma^m]_{\ell-1, \ell}^* - [M_m^{-1} \gamma^m]_{\ell, \ell-1} \right) \right. \\ \left. + 2i \sum_{\ell''=|m|} \frac{[M_m^{-1} \gamma^m]_{\ell-1, \ell''}^* [M_m^{-1} \gamma^m]_{\ell, \ell''}}{k r_0^2 f(r_0) |v_{\ell''}(r_0)|^2} \right] \quad (39)$$

where $m \in \mathbb{Z}$, $\ell \in \mathbb{N}_0$ and we have changed the overall sign in order to obtain the force acting on the system.

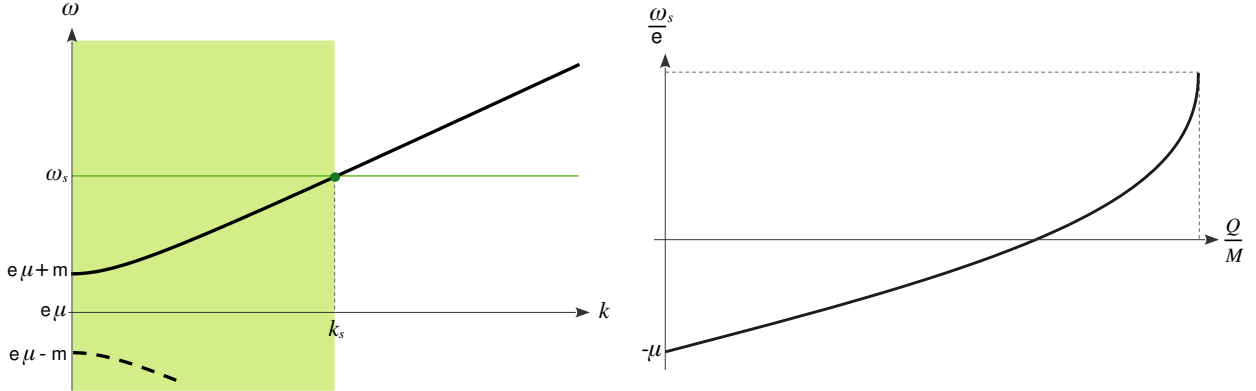


FIG. 3: Superradiant phenomenon. Left: Plane wave frequency ω_{\pm} and superradiant frequency. The green region is the superradiant region and the green dot mark the intersection at k_s . Right: Behavior of the superradiance frequency ω_s with the ratio Q/M and the charge e

C. Numerical Results

The numerical analysis of the force (39) starts by noticing that it depends on the same classical pieces as in Sec. III D, *i.e.* the inverse operator M_m^{-1} , the matrices γ^m and the radial solutions evaluated at the mirror radius.

To understand how superradiance works, we plot in Fig. 3 (left) the dispersion relation $\omega_{\pm} = \pm\sqrt{k^2 + m^2} - e\mu$ as compared to the superradiant frequency ω_s . The intersection at $k = k_s$ divides the k axis into two regions: For $k \geq k_s$ we have no superradiance and we expect to have a positive thrust force (pushing the mirror upwards). For $k \leq k_s$ on the other hand, the system superradiates and thus we expect a negative thrust force (pushing the mirror downwards). Moreover, in Fig. 3 (right) we plot the superradiant frequency ω_s as a function of the black hole charge, showing that it is maximal for the extremal black hole, while it goes to $-\mu$ in the Schwarzschild limit.

We start by calculating the thrust without any black hole, corresponding to an isotropic superposition of modes with momentum k . As anticipated in sec III D, we get a non-vanishing background force, see Fig. 4. This happens because the mirror at rest is not in thermodynamic equilibrium with the thermal bath. As it is accelerated through the bath, the force eventually equilibrates with the drag on the opposite side, resulting in an equilibrium state in which the mirror moves with constant velocity. The background force depends on the parameters T and μ , being not sensitive to the particle mass m or charge e .

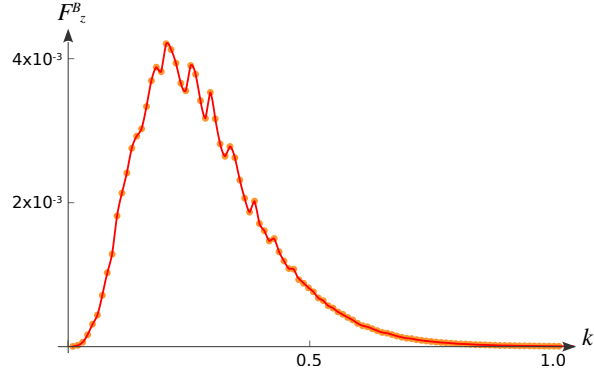


FIG. 4: Thrust force without the black hole $M = 0$, $Q = 0$. This plot corresponds to $m = 0.1$, $e = 3m$, $\mu = -0.01$, $T = 0.07$. The points represent the values of the integrand in (39) as a function of k , and the resulting thrust force is given the area under the interpolating curve.

We move now to the case in which a charged black hole sits at the centre of the geometry. In Fig. 5 we show the thrust force for two different black holes, from which the background contribution has been subtracted. We consider one case which is not favorable to superradiance (left) and another one with a large superradiance region (right). As it could have been expected, there is a change of sign in the resulting force as we move into the superradiance region. These plots correspond to an isotropic superposition of modes with fixed k , the total thrust corresponding to the integral over k . We see that in the less superradiant case the total area below the curve is positive, while in the more superradiant case it is negative.

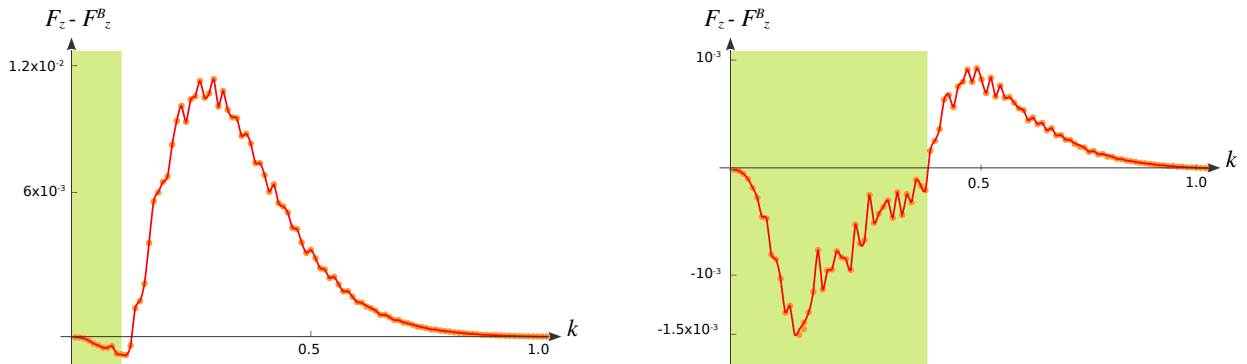


FIG. 5: Black hole thrust force obtained by removing the background. The green regions are superradiant. These plots correspond to $r_0 = 5r_+$, $m = 0.1$, $e = 3m$, $\mu = -0.01$, $T = 0.07$. The points represent the values of the integrand in (39) as a function of k , and the resulting thrust force is given the integral under the interpolating curve.

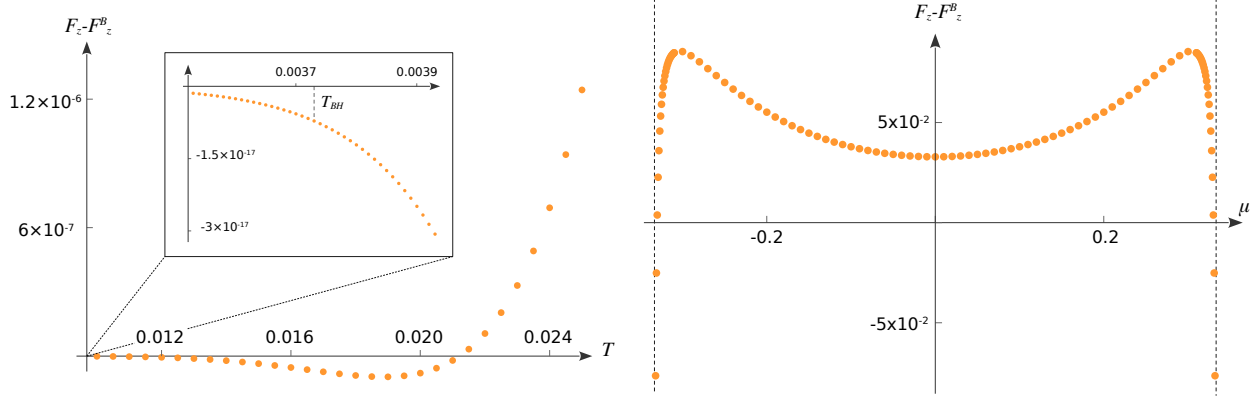


FIG. 6: Thrust force as a function of the thermal bath parameters, with the same background parameters as in Fig. 5.

These results imply that it is possible to use the superradiant process to effectively build a “superradiant black hole rocket”. As we discuss in what follows, the rocket parameters can be optimized to maximize the resulting thrust.

The parameters of the thermal bath T and μ only appear in the force (39) through the prefactor containing the Bose-Einstein distribution. This dependence is easy to analyze with the help of the plots in Fig. 5. Indeed, since the modes with small k have a larger weight for lower the temperatures, we can always get a negative (superradiant) total force. This can be seen in the plot in Fig. 6 (left). On the other hand, the modes with smaller k get a larger weight as the chemical potential approaches its limiting values $\pm|m|/e$. This results in a change of sign of the total force as the superradiant region become dominant, see the plot in Fig. 6 (right).

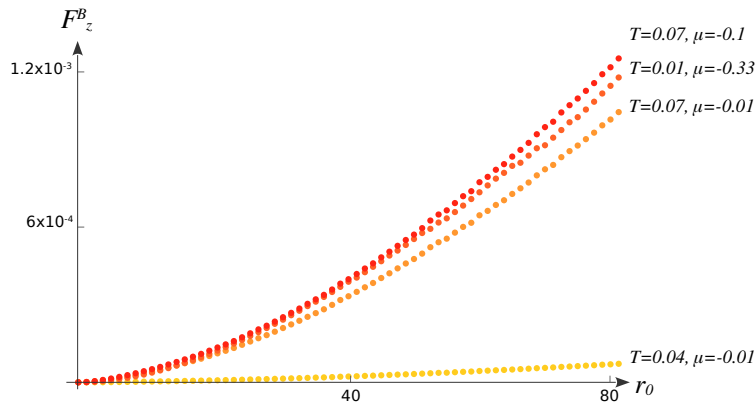


FIG. 7: Background force for different thermal baths and mirror radii, from $r_0 = 0.1$ to $r_0 = 80$.

Lastly, we studied the variation of the thrust as a function of the mirror radius r_0 . We first plot in Fig. 7 the background force without the black hole, as a function of the mirror radius and for different values of the thermal parameters. As expected, it vanishes at $r_0 = 0$ and grows monotonically with r_0 . Then, in Fig. 8 we obtain the thrust force in the presence of the black hole, varying the mirror radius r_0 for different values of the temperature T and chemical potential μ . We see that the sign of the force can change with the radius and, more interestingly, a set of peaks appear for discrete and approximately evenly spaced radii.

To further understand such “resonant” modes, in Fig. 9 we plot the force (39) for an isotropic superposition of modes with a fixed value of k as a function of the mirror radius. We see that the resulting peaks coincide almost perfectly with the zeros of the radial function $u_\ell(r)$. This supports the interpretation of the peaks as due to the modes that would resonate on a closed cavity with similar radius. For a more detailed analysis, see Appendix B 4.

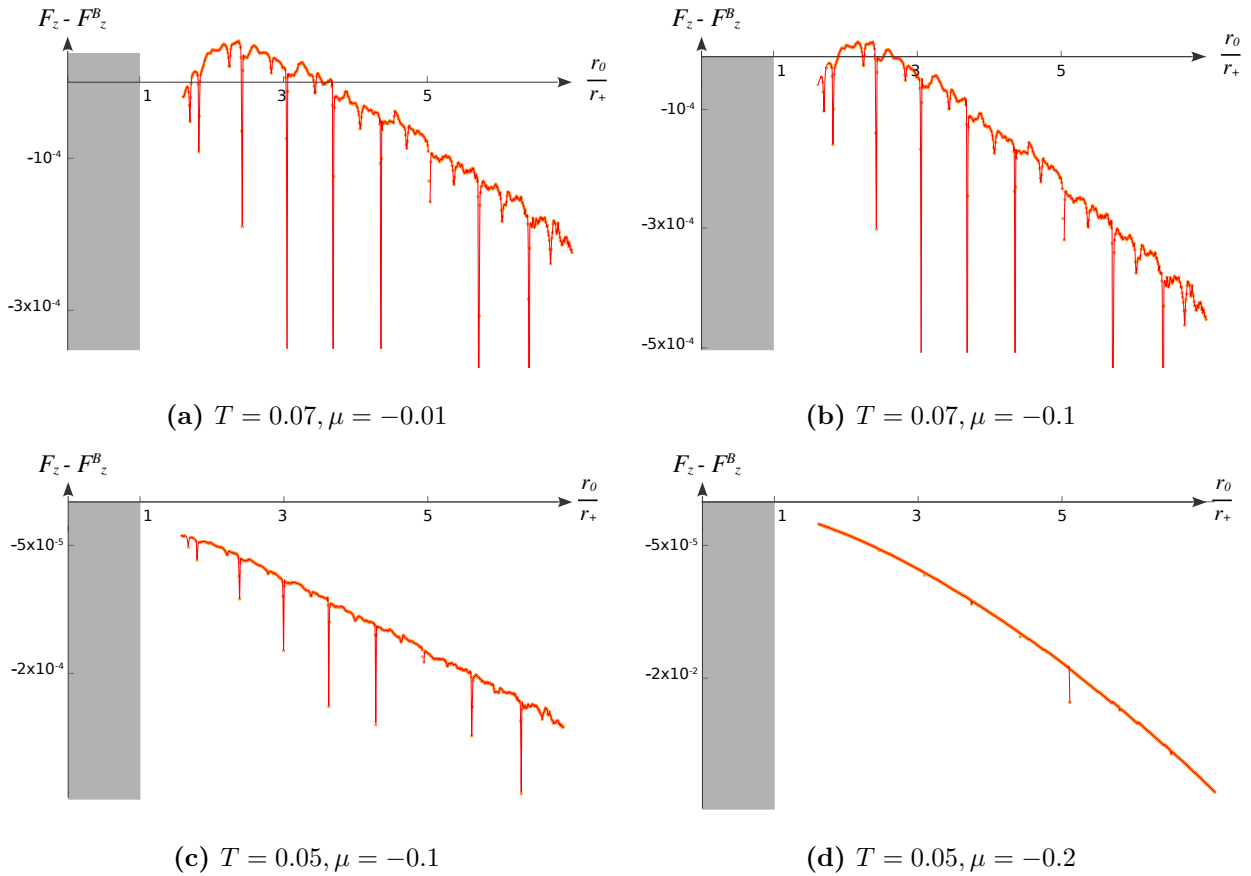


FIG. 8: Total thrust force obtained as a function of the mirror radius r_0 normalized with the horizon r_+ at different T and μ . Here we fix $Q = 0.99M$ and $e = 5m$.

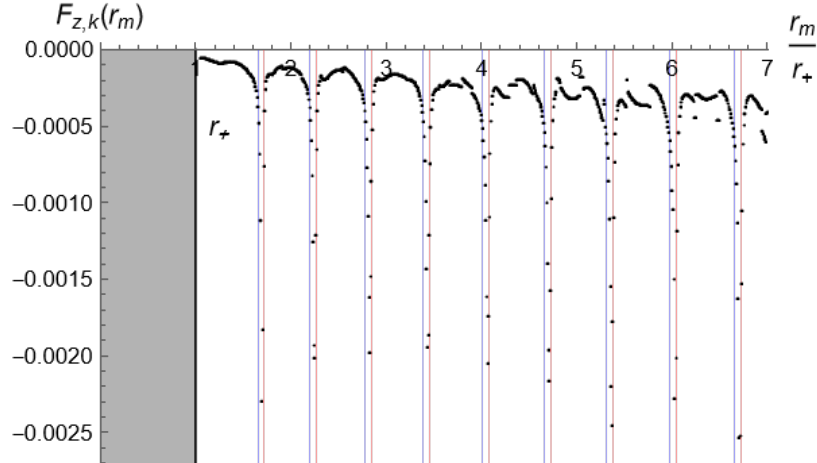


FIG. 9: Total thrust force obtained as function of the mirror radius r_0 normalized with the horizon r_+ at $k = 0.37$. Here we fix $Q = 0.99M$, $e = 5m$, $T = 0.07$ and $\mu = -0.01$. The blue and red lines correspond to the zeros of $\Re[u_\ell(r)]$ and $\Im[u_\ell(r)]$ respectively for $\ell = 0$.

V. DISCUSSION

In this note, we calculated the thrust on a semi-spherical mirror centered around a charged black hole, which is immersed in a thermal bath made of charged scalar particles. We dubbed the system a “black hole superradiant rocket”

We obtained the resulting force as a function of the black hole parameters mass and charge, the thermal bath parameters temperature and chemical potential, and the rocket parameter corresponding to the mirror radius. We compared it with the equilibration thrust that we would obtain in the absence of the black hole.

We found that within the superradiant regime there is a net force acting on the system, originated on the superradiant modes. Furthermore, we identified that by fine-tuning external and rocket parameters, this force can be optimized to maximize its value. Particularly noteworthy are the resonant peaks in the thrust profile, reminiscent of the well-known “black hole bomb” modes [10]. Leveraging these resonances by adjusting the mirror’s radius to coincide with one of these peaks allows for the extraction of maximum thrust.

A future research direction may involve extending the calculations to a spin 1/2 field, representing matter. This would allow for the evaluation of the magnitude of thrust under realistic parameter values. Indeed, since this works as a toy model of Kerr black holes, a possible application could be on observables of primordial black holes superradiance [11–13].

Appendix A: Energy-Momentum Tensor

The Lagrangian of a free complex scalar field is given by:

$$\mathcal{L} =: (\partial_\alpha \hat{\Phi})(\partial^\alpha \hat{\Phi}^\dagger) - m^2 \hat{\Phi} \hat{\Phi}^\dagger : \quad (\text{A1})$$

From this we can compute its energy-momentum tensor:

$$\begin{aligned} T_{\mu\nu} &= \frac{\partial \mathcal{L}}{\partial(\partial^\mu \hat{\Phi})} \partial_\nu \hat{\Phi} + \frac{\partial \mathcal{L}}{\partial(\partial^\mu \hat{\Phi}^\dagger)} \partial_\nu \hat{\Phi}^\dagger - g_{\mu\nu} \mathcal{L} \\ &= (\partial_\mu \partial'_\nu + \partial'_\mu \partial_\nu - g_{\mu\nu} (\partial'_\alpha \partial^\alpha - m^2)) \left(: \hat{\Phi}^\dagger(\mathbf{x}) \hat{\Phi}(\mathbf{x}') : \right) |_{\mathbf{x}'=\mathbf{x}} \end{aligned} \quad (\text{A2})$$

where we write $\partial_\mu \hat{\Phi}(\mathbf{x}) = \partial'_\mu \hat{\Phi}(\mathbf{x}')|_{\mathbf{x}'=\mathbf{x}}$ in order to simplify the notation. However, since we are interested in a thermal bath of particles and antiparticles at temperature T and chemical potential μ , then it will be more useful to take the mean value of the energy-momentum tensor:

$$T_{\mu\nu} = \frac{1}{2} (\partial_\mu \partial'_\nu + \partial'_\mu \partial_\nu - g_{\mu\nu} (\partial'_\alpha \partial^\alpha - m^2)) \langle : \hat{\Phi}^\dagger(\mathbf{x}) \hat{\Phi}(\mathbf{x}') : \rangle |_{\mathbf{x}'=\mathbf{x}} \quad (\text{A3})$$

the prefactor 1/2 is to avoid double counting. Finally, we couple the gauge field,

$$\begin{cases} \partial_\mu \hat{\Phi}^\dagger(\mathbf{x}) \longrightarrow \partial_\mu \hat{\Phi}^\dagger(\mathbf{x}) + ieA_\mu \hat{\Phi}^\dagger(\mathbf{x}) \\ \partial'_\mu \hat{\Phi}(\mathbf{x}') \longrightarrow \partial'_\mu \hat{\Phi}(\mathbf{x}') - ieA'_\mu \hat{\Phi}(\mathbf{x}') \end{cases} \quad (\text{A4})$$

and obtain the energy-momentum tensor:

$$\begin{aligned} T_{\mu\nu} &= \frac{1}{2} \left((\partial_\mu + ieA_\mu)(\partial'_\nu - ieA'_\nu) + (\partial'_\mu - ieA'_\mu)(\partial_\nu + ieA_\nu) \right. \\ &\quad \left. - g_{\mu\nu} ((\partial'_\alpha - ieA'_\alpha)(\partial^\alpha + ieA^\alpha) - m^2) \right) \langle : \hat{\Phi}^\dagger(\mathbf{x}) \hat{\Phi}(\mathbf{x}') : \rangle |_{\mathbf{x}'=\mathbf{x}} \end{aligned} \quad (\text{A5})$$

Now, for the calculation of the thrust force in sec IV B we only need to compute T_{rr} and $T_{r\theta}$ in the limit $r \rightarrow \infty$. In this limit, the gauge field will be just $A_\mu = A'_\mu = \mu$, then for the components of interest we have:

$$\begin{aligned} T_{rr} &= \frac{1}{2} \left(\partial'_t \partial_t + ie\mu(\partial'_t - \partial_t) + \partial_r \partial'_r - \frac{1}{r^2} \partial'_\theta \partial_\theta - \frac{1}{r^2 \sin^2(\theta)} \partial'_\phi \partial_\phi - m^2 + e^2 \mu^2 \right) \times \\ &\quad \times \langle : \hat{\Phi}^\dagger(\mathbf{x}) \hat{\Phi}(\mathbf{x}') : \rangle |_{\mathbf{x}'=\mathbf{x}} \end{aligned} \quad (\text{A6})$$

$$T_{r\theta} = \frac{1}{2} (\partial_r \partial'_\theta + \partial'_r \partial_\theta) \langle : \hat{\Phi}^\dagger(\mathbf{x}) \hat{\Phi}(\mathbf{x}') : \rangle |_{\mathbf{x}'=\mathbf{x}} \quad (\text{A7})$$

Therefore, in order to obtain these components of the energy-momentum tensor, it only remains to obtain the expected value of the fields $\langle : \hat{\Phi}^\dagger(\mathbf{x}) \hat{\Phi}(\mathbf{x}') : \rangle$. Since we are computing

the energy-momentum tensor at infinity, the field at infinity is given by two contributions $\hat{\Phi} = \hat{\Phi}^{\text{inc}} + \hat{\Phi}^{\text{scatt}}$, the incident and the scattered components at infinity. Thus, we can use this contributions of the field to separate the expectation value as:

$$\begin{aligned} \langle : \hat{\Phi}^\dagger(\mathbf{x})\hat{\Phi}(\mathbf{x}') : \rangle |_{\mathbf{x}'=\mathbf{x}} = & \left[\langle : \hat{\Phi}^{\text{scatt}\dagger}(\mathbf{x})\hat{\Phi}^{\text{scat}}(\mathbf{x}') : \rangle + \langle : \hat{\Phi}^{\text{scatt}\dagger}(\mathbf{x})\hat{\Phi}^{\text{inc}}(\mathbf{x}') : \rangle \right. \\ & \left. + \langle : \hat{\Phi}^{\text{inc}\dagger}(\mathbf{x})\hat{\Phi}^{\text{scat}}(\mathbf{x}') : \rangle + \langle : \hat{\Phi}^{\text{inc}\dagger}(\mathbf{x})\hat{\Phi}^{\text{inc}}(\mathbf{x}') : \rangle \right] |_{\mathbf{x}'=\mathbf{x}} \quad (\text{A8}) \end{aligned}$$

where the pure incident field term vanishes when we integrate in all directions (its the total force without the mirror). In the same way, the momentum energy tensor can be separated by writing:

$$\begin{cases} T_{rr} = T_{rr}^{\text{scat/scat}} + T_{rr}^{\text{scat/inc}} + T_{rr}^{\text{inc/scat}} \\ T_{r\theta} = T_{r\theta}^{\text{scat/scat}} + T_{r\theta}^{\text{scat/inc}} + T_{r\theta}^{\text{inc/scat}} \end{cases} \quad (\text{A9})$$

In order to obtain each of this terms, we will need the fields expectation value, but first we will compute the mean value between the operators \hat{b}_ℓ^m and \hat{c}_ℓ^m which are present in the field definitions (14).

1. Mean values between operators \hat{b}_ℓ^m and \hat{c}_ℓ^m

Starting from the definition of the incident field operator (13) but using the normalization of the quantum field (31):

$$\hat{c}_\ell^m = \frac{\omega_+ + \mathbf{e}\mu}{2\pi^2\sqrt{|\omega_+\omega_-|}} \frac{e^{i\frac{\pi}{2}\ell}}{\sqrt{2\omega_+}} \hat{A}_{\vec{k}} Y_\ell^{m*}(\tilde{n}) w_\ell(r_0) \quad (\text{A10})$$

and its analogue for antiparticles,

$$\hat{\tilde{c}}_\ell^m = \frac{\omega_+ + \mathbf{e}\mu}{2\pi^2\sqrt{|\omega_+\omega_-|}} \frac{e^{i\frac{\pi}{2}\ell}}{\sqrt{-2\omega_-}} \hat{B}_{\vec{k}} Y_\ell^{m*}(\tilde{n}) w_\ell(r_0) \quad (\text{A11})$$

where we used $|\omega_\pm + \mathbf{e}\mu| = \omega_+ + \mathbf{e}\mu$. We can immediately obtain the expectation value of the quadratic operator $\hat{c}_\ell^{m\dagger}\hat{c}_\ell^m$ over all directions of incidence:

$$\begin{aligned} \int d\tilde{n} d\tilde{n}' \langle \hat{c}_\ell^{m\dagger}\hat{c}_{\ell'}^{m'} \rangle = & \int d\tilde{n} d\tilde{n}' \frac{e^{i\frac{\pi}{2}(\ell'-\ell)}}{(2\pi^2)^2\sqrt{2\omega_+}\sqrt{2\omega'_+}} \frac{(\omega_+ + \mathbf{e}\mu)(\omega'_+ + \mathbf{e}\mu)}{\sqrt{|\omega_+\omega_-|}\sqrt{|\omega'_+\omega'_-|}} \times \\ & \times Y_\ell^m(\tilde{n}) Y_{\ell'}^{m'*}(\tilde{n}') w_\ell^*(r_0) w_{\ell'}(r_0) \langle \hat{A}_{\vec{k}}^\dagger \hat{A}_{\vec{k}'} \rangle \end{aligned} \quad (\text{A12})$$

Using the Bose-Einstein distribution (32) and writing the Dirac delta in spherical coordinates,

$$\int d\tilde{n} d\tilde{n}' \langle \hat{c}_\ell^{m\dagger} \hat{c}_{\ell'}^{m'} \rangle = \int d\tilde{n} d\tilde{n}' \frac{e^{i\frac{\pi}{2}(\ell'-\ell)}}{\pi\sqrt{\omega_+}\sqrt{\omega'_+}} \frac{(\omega_+ + \mathbf{e}\mu)(\omega'_+ + \mathbf{e}\mu)}{\sqrt{|\omega_+\omega_-|}\sqrt{|\omega'_+\omega'_-|}} \times \quad (\text{A13})$$

$$\times Y_\ell^m(\tilde{n}) Y_{\ell'}^{m'*}(\tilde{n}') \frac{w_\ell^*(r_0)w_{\ell'}(r_0)}{e^{\frac{\omega_\pm}{T}} - 1} \frac{\delta(k-k')}{k^2} \frac{\delta(\theta-\theta')\delta(\phi-\phi')}{\sin(\theta)}$$

The integral is over all the possible directions but not over k , then by doing the angular integration it remains:

$$\int d\tilde{n} d\tilde{n}' \langle \hat{c}_\ell^{m\dagger} \hat{c}_{\ell'}^{m'} \rangle = \frac{(\omega_+ + \mathbf{e}\mu)^2}{\pi |\omega_+\omega_-|} \frac{|w_\ell(r_0)|^2}{\omega_+ \left(e^{\frac{\omega_\pm}{T}} - 1 \right)} \frac{\delta(k-k')}{k^2} \delta_{\ell\ell'} \delta_{mm'} \quad (\text{A14})$$

Proceeding in the same way for antiparticles, the expectation value of the quadratic operator is obtained considering all directions of incidence, where the change of sign in the exponential is due to the change in the Bose-Einstein distribution:

$$\int d\tilde{n} d\tilde{n}' \langle \hat{c}_\ell^{m\dagger} \hat{c}_{\ell'}^{m'} \rangle = -\frac{(\omega_+ + \mathbf{e}\mu)^2}{\pi |\omega_+\omega_-|} \frac{|w_\ell(r_0)|^2}{\omega_- \left(e^{-\frac{\omega_\pm}{T}} - 1 \right)} \frac{\delta(k-k')}{k^2} \delta_{\ell\ell'} \delta_{mm'} \quad (\text{A15})$$

Moreover, using the result (A14) and the classical result (29) we can obtain the mean value between \hat{c}_ℓ^m and \hat{b}_ℓ^m over all directions:

$$\int d\tilde{n} d\tilde{n}' \langle \hat{c}_\ell^{m\dagger} \hat{b}_{\ell'}^{m'} \rangle = \int d\tilde{n} d\tilde{n}' \langle \hat{c}_\ell^{m\dagger} \sum_{\ell''=|m'|}^{\infty} \hat{c}_{\ell''}^{m'} O_{\ell'\ell''} \rangle = \sum_{\ell''=|m'|}^{\infty} O_{\ell'\ell''} \int d\tilde{n} d\tilde{n}' \langle \hat{c}_\ell^{m\dagger} \hat{c}_{\ell''}^{m'} \rangle \quad (\text{A16})$$

$$= O_{\ell'\ell} \frac{(\omega_+ + \mathbf{e}\mu)^2}{\pi |\omega_+\omega_-|} \frac{|w_\ell(r_0)|^2}{\omega_+ \left(e^{\frac{\omega_\pm}{T}} - 1 \right)} \frac{\delta(k-k')}{k^2} \delta_{mm'}$$

Analogously, other useful results are obtained:

$$\int d\tilde{n} d\tilde{n}' \langle \hat{b}_\ell^{m\dagger} \hat{c}_{\ell'}^{m'} \rangle = O_{\ell\ell'}^* \frac{(\omega_+ + \mathbf{e}\mu)^2}{\pi |\omega_+\omega_-|} \frac{|w_{\ell'}(r_0)|^2}{\omega_+ \left(e^{\frac{\omega_\pm}{T}} - 1 \right)} \frac{\delta(k-k')}{k^2} \delta_{m'm} \quad (\text{A17})$$

$$\int d\tilde{n} d\tilde{n}' \langle \hat{b}_\ell^{m\dagger} \hat{b}_{\ell'}^{m'} \rangle = \sum_{\ell''=|m|}^{\infty} O_{\ell\ell''}^* O_{\ell'\ell''} \frac{(\omega_+ + \mathbf{e}\mu)^2}{\pi |\omega_+\omega_-|} \frac{|w_{\ell''}(r_0)|^2}{\omega_+ \left(e^{\frac{\omega_\pm}{T}} - 1 \right)} \frac{\delta(k-k')}{k^2} \delta_{mm'} \quad (\text{A18})$$

In addition, we obtain the same expressions between the antiparticles operators \hat{c}_ℓ^m and \hat{b}_ℓ^m by using (A15).

$$\int d\tilde{n} d\tilde{n}' \langle \hat{c}_\ell^{m\dagger} \hat{b}_{\ell'}^{m'} \rangle = -O_{\ell'\ell} \frac{(\omega_+ + \mathbf{e}\mu)^2}{\pi |\omega_+\omega_-|} \frac{|w_\ell(r_0)|^2}{\omega_- \left(e^{-\frac{\omega_\pm}{T}} - 1 \right)} \frac{\delta(k-k')}{k^2} \delta_{mm'} \quad (\text{A19})$$

$$\int d\tilde{n} d\tilde{n}' \langle \hat{b}_\ell^{m\dagger} \hat{c}_{\ell'}^{m'} \rangle = -O_{\ell\ell'}^* \frac{(\omega_+ + \mathbf{e}\mu)^2}{\pi |\omega_+ \omega_-|} \frac{|w_{\ell'}(r_0)|^2}{\omega_- \left(e^{-\frac{\omega_-}{T}} - 1 \right)} \frac{\delta(k - k')}{k^2} \delta_{m'm} \quad (\text{A20})$$

$$\int d\tilde{n} d\tilde{n}' \langle \hat{b}_\ell^{m\dagger} \hat{b}_{\ell'}^{m'} \rangle = - \sum_{\ell''=|m|}^{\infty} O_{\ell\ell''}^* O_{\ell'\ell''} \frac{(\omega_+ + \mathbf{e}\mu)^2}{\pi |\omega_+ \omega_-|} \frac{|w_{\ell''}(r_0)|^2}{\omega_- \left(e^{-\frac{\omega_-}{T}} - 1 \right)} \frac{\delta(k - k')}{k^2} \delta_{mm'} \quad (\text{A21})$$

We then have the needed tools to compute the expectation values of the fields.

2. Expectation values $\langle : \hat{\Phi}^\dagger(\mathbf{x}) \hat{\Phi}(\mathbf{x}') : \rangle$

The quantized version of the classical fields obtained in sec III B are:

$$\hat{\Phi}^{\text{scat}}(r, \theta, \phi, t) = \int_{\infty}^{\infty} d^3k \sum_{\ell, m} \left(e^{-i\omega_+ t} \hat{b}_\ell^m \frac{v_\ell(r)}{v_\ell(r_0)} Y_\ell^m(\theta, \phi) + e^{-i\omega_- t} \hat{b}_\ell^{m\dagger} \frac{v_\ell^*(r)}{v_\ell^*(r_0)} Y_\ell^{m*}(\theta, \phi) \right) \quad (\text{A22})$$

$$\hat{\Phi}^{\text{inc}}(r, \theta, \phi, t) = \int_{\infty}^{\infty} d^3k \sum_{\ell, m} \left(e^{-i\omega_+ t} \hat{c}_\ell^m \frac{w_\ell(r)}{w_\ell(r_0)} Y_\ell^m(\theta, \phi) + e^{-i\omega_- t} \hat{c}_\ell^{m\dagger} \frac{w_\ell^*(r)}{w_\ell^*(r_0)} Y_\ell^{m*}(\theta, \phi) \right) \quad (\text{A23})$$

First we obtain $\langle : \hat{\Phi}^{\text{scat}\dagger}(\mathbf{x}) \hat{\Phi}^{\text{scat}}(\mathbf{x}') : \rangle$, then replacing with (A22) and expanding the product we have:

$$\begin{aligned} \langle : \hat{\Phi}^{\text{scat}\dagger}(\mathbf{x}) \hat{\Phi}^{\text{scat}}(\mathbf{x}') : \rangle &= \int d^3k d^3k' \sum_{\ell, m} \sum_{\ell', m'} \times \\ &\times \left[e^{i(\omega_+ t - \omega'_+ t')} \frac{v_\ell^*(r) v_{\ell'}(r')}{v_\ell^*(r_0) v_{\ell'}(r_0)} Y_\ell^{m*}(\theta, \phi) Y_{\ell'}^m(\theta', \phi') \langle \hat{b}_\ell^{m\dagger} \hat{b}_{\ell'}^{m'} \rangle \right. \\ &\left. + e^{-i(-\omega_- t + \omega'_- t')} \frac{v_\ell(r) v_{\ell'}^*(r')}{v_\ell(r_0) v_{\ell'}^*(r_0)} Y_\ell^m(\theta, \phi) Y_{\ell'}^{m'*}(\theta', \phi') \langle \hat{b}_{\ell'}^{m'\dagger} \hat{b}_\ell^m \rangle \right] \end{aligned} \quad (\text{A24})$$

where we used that the only non zero mean value is $\langle \hat{b}_\ell^{m\dagger} \hat{b}_{\ell'}^{m'} \rangle$ (as discussed in sec A 1). Also, using spherical coordinates we can use the angular integral (A18), obtaining then the mean value of the fields:

$$\begin{aligned} \langle : \hat{\Phi}^{\text{scat}\dagger}(\mathbf{x}) \hat{\Phi}^{\text{scat}}(\mathbf{x}') : \rangle &= \int dk \frac{(\omega_+ + \mathbf{e}\mu)^2 k^2}{\pi |\omega_+ \omega_-|} \sum_{\ell, \ell', m} \sum_{\ell'', m''=|m|} |w_{\ell''}(r_0)|^2 \times \\ &\times \left[e^{i\omega_+(t-t')} \frac{v_\ell^*(r) v_{\ell'}(r')}{v_\ell^*(r_0) v_{\ell'}(r_0)} \frac{Y_\ell^{m*}(\theta, \phi) Y_{\ell'}^m(\theta', \phi') O_{\ell\ell''}^* O_{\ell'\ell''}}{\omega_+ \left(e^{\frac{\omega_+}{T}} - 1 \right)} \right. \\ &\left. - e^{i\omega_-(t-t')} \frac{v_\ell(r) v_{\ell'}^*(r')}{v_\ell(r_0) v_{\ell'}^*(r_0)} \frac{Y_\ell^m(\theta, \phi) Y_{\ell'}^{m*}(\theta', \phi') O_{\ell'\ell''}^* O_{\ell\ell''}}{\omega_- \left(e^{-\frac{\omega_-}{T}} - 1 \right)} \right] \end{aligned} \quad (\text{A25})$$

In the same way we can obtain the expectation value $\langle : \hat{\Phi}^{\text{scat}\dagger}(\mathbf{x}) \hat{\Phi}^{\text{inc}}(\mathbf{x}') : \rangle$, then replacing with (A22) and (A23) we have:

$$\begin{aligned} \langle : \hat{\Phi}^{\text{scat}\dagger}(\mathbf{x}) \hat{\Phi}^{\text{inc}}(\mathbf{x}') : \rangle &= \int d^3k d^3k' \sum_{\ell, m} \sum_{\ell', m'} \times \\ &\times \left[e^{i(\omega_+ t - \omega'_+ t')} \frac{v_\ell^*(r) w_{\ell'}(r')}{v_\ell^*(r_0) w_{\ell'}(r_0)} Y_\ell^{m*}(\theta, \phi) Y_{\ell'}^{m'}(\theta', \phi') \langle \hat{b}_\ell^{m\dagger} \hat{c}_{\ell'}^{m'} \rangle \right. \\ &\left. + e^{-i(-\omega_- t + \omega'_- t')} \frac{v_\ell(r) w_{\ell'}^*(r')}{v_\ell(r_0) w_{\ell'}^*(r_0)} Y_\ell^m(\theta, \phi) Y_{\ell'}^{m'*}(\theta', \phi') \langle \hat{c}_{\ell'}^{m'\dagger} \hat{b}_\ell^m \rangle \right] \end{aligned} \quad (\text{A26})$$

Using the angular integrals (A16) and (A17), we then obtain the expectation value of the fields:

$$\begin{aligned} \langle : \hat{\Phi}^{\text{scat}\dagger}(\mathbf{x}) \hat{\Phi}^{\text{inc}}(\mathbf{x}') : \rangle &= \int dk \frac{(\omega_+ + \mathbf{e}\mu)^2 k^2}{\pi |\omega_+ \omega_-|} \sum_{\ell, m, \ell'} |w_{\ell'}(r_0)|^2 \times \\ &\times \left[e^{i\omega_+(t-t')} \frac{v_\ell^*(r) w_{\ell'}(r')}{v_\ell^*(r_0) w_{\ell'}(r_0)} \frac{Y_\ell^{m*}(\theta, \phi) Y_{\ell'}^m(\theta', \phi') O_{\ell\ell'}^*}{\omega_+ \left(e^{\frac{\omega_+}{T}} - 1 \right)} \right. \\ &\left. - e^{i\omega_-(t-t')} \frac{v_\ell(r) w_{\ell'}^*(r')}{v_\ell(r_0) w_{\ell'}^*(r_0)} \frac{Y_\ell^m(\theta, \phi) Y_{\ell'}^{m*}(\theta', \phi') O_{\ell\ell'}}{\omega_- \left(e^{-\frac{\omega_-}{T}} - 1 \right)} \right] \end{aligned} \quad (\text{A27})$$

Finally, we proceed in the same way for $\langle : \hat{\Phi}^{\text{inc}\dagger}(\mathbf{x}) \hat{\Phi}^{\text{scat}}(\mathbf{x}') : \rangle$, so replacing with (A22) and (A23) we have:

$$\begin{aligned} \langle : \hat{\Phi}^{\text{inc}\dagger}(\mathbf{x}) \hat{\Phi}^{\text{scat}}(\mathbf{x}') : \rangle &= \int d^3k d^3k' \sum_{\ell, m} \sum_{\ell', m'} \times \\ &\times \left[e^{i(\omega_+ t - \omega'_+ t')} \frac{w_\ell^*(r) v_{\ell'}(r')}{w_\ell^*(r_0) v_{\ell'}(r_0)} Y_\ell^{m*}(\theta, \phi) Y_{\ell'}^{m'}(\theta', \phi') \langle \hat{c}_\ell^{m\dagger} \hat{b}_{\ell'}^{m'} \rangle \right. \\ &\left. + e^{-i(-\omega_- t + \omega'_- t')} \frac{w_\ell(r) v_{\ell'}^*(r')}{w_\ell(r_0) v_{\ell'}^*(r_0)} Y_\ell^m(\theta, \phi) Y_{\ell'}^{m'*}(\theta', \phi') \langle \hat{b}_{\ell'}^{m'\dagger} \hat{c}_\ell^m \rangle \right] \end{aligned} \quad (\text{A28})$$

Using the angular integrals (A16) and (A17), we then obtain the expectation value of the fields:

$$\begin{aligned} \langle : \hat{\Phi}^{\text{inc}\dagger}(\mathbf{x}) \hat{\Phi}^{\text{scat}}(\mathbf{x}') : \rangle &= \int dk \frac{(\omega_+ + \mathbf{e}\mu)^2 k^2}{\pi |\omega_+ \omega_-|} \sum_{\ell, m, \ell'} |w_\ell(r_0)|^2 \times \\ &\times \left[e^{i\omega_+(t-t')} \frac{w_\ell^*(r) v_{\ell'}(r')}{w_\ell^*(r_0) v_{\ell'}(r_0)} \frac{Y_\ell^{m*}(\theta, \phi) Y_{\ell'}^m(\theta', \phi') O_{\ell\ell'}}{\omega_+ \left(e^{\frac{\omega_+}{T}} - 1 \right)} \right. \\ &\left. - e^{i\omega_-(t-t')} \frac{w_\ell(r) v_{\ell'}^*(r')}{w_\ell(r_0) v_{\ell'}^*(r_0)} \frac{Y_\ell^m(\theta, \phi) Y_{\ell'}^{m*}(\theta', \phi') O_{\ell\ell'}^*}{\omega_- \left(e^{-\frac{\omega_-}{T}} - 1 \right)} \right] \end{aligned} \quad (\text{A29})$$

We can now continue with the computation of each term of the energy-momentum tensor in (A9).

3. Computation of T_{rr}

We obtain the component T_{rr} of the energy-momentum tensor separating the different field contributions:

$$T_{rr} = T_{rr}^{\text{scat/scat}} + T_{rr}^{\text{scat/inc}} + T_{rr}^{\text{inc/scat}} \quad (\text{A30})$$

where each of this part satisfies the definition (A6):

$$T_{rr} = \frac{1}{2} \left(\partial'_t \partial_t + i\mathbf{e}\mu(\partial'_t - \partial_t) + \partial_r \partial'_r - \frac{1}{r^2} \partial'_\theta \partial_\theta - \frac{1}{r^2 \sin^2(\theta)} \partial'_\phi \partial_\phi - \mathbf{m}^2 + \mathbf{e}^2 \mu^2 \right) \times \langle : \hat{\Phi}^\dagger(\mathbf{x}) \hat{\Phi}(\mathbf{x}') : \rangle |_{\mathbf{x}'=\mathbf{x}} \quad (\text{A31})$$

Now we need to replace with each fields expectation value computed in sec A 2. Beginning with $T_{rr}^{\text{scat/scat}}$, we will use the result (A25):

$$T_{rr}^{\text{scat/scat}} = \frac{1}{2} \left(\partial'_t \partial_t + i\mathbf{e}\mu(\partial'_t - \partial_t) + \partial_r \partial'_r - \frac{1}{r^2} \partial'_\theta \partial_\theta - \frac{1}{r^2 \sin^2(\theta)} \partial'_\phi \partial_\phi - \mathbf{m}^2 + \mathbf{e}^2 \mu^2 \right) \times \langle : \hat{\Phi}^{\text{scat}\dagger}(\mathbf{x}) \hat{\Phi}^{\text{scat}}(\mathbf{x}') : \rangle |_{\mathbf{x}'=\mathbf{x}} \quad (\text{A32})$$

since we are interesting in the limit $r \rightarrow \infty$, the angular derivatives will vanish at leader order (since the angular dependence are only in the spherical harmonics). First we will obtain the terms with time derivatives ∂_t :

$$\begin{aligned} \partial'_t \partial_t \langle : \hat{\Phi}^{\text{scat}\dagger}(\mathbf{x}) \hat{\Phi}^{\text{scat}}(\mathbf{x}') : \rangle &= \int dk \frac{(\omega_+ + \mathbf{e}\mu)^2 k^2}{\pi |\omega_+ \omega_-|} \sum_{\ell, \ell', m} \sum_{\ell''=|m|} |w_{\ell\ell''}(r_0)|^2 \times \\ &\times \left[\omega_+^2 e^{i\omega_+(t-t')} \frac{v_\ell^*(r) v_{\ell'}(r')}{v_\ell^*(r_0) v_{\ell'}(r_0)} \frac{Y_\ell^{m*}(\theta, \phi) Y_{\ell'}^m(\theta', \phi') O_{\ell\ell''}^* O_{\ell'\ell''}}{\omega_+ \left(e^{\frac{\omega_+}{T}} - 1 \right)} \right. \\ &\left. - \omega_-^2 e^{i\omega_-(t-t')} \frac{v_\ell(r) v_{\ell'}^*(r')}{v_\ell(r_0) v_{\ell'}^*(r_0)} \frac{Y_\ell^m(\theta, \phi) Y_{\ell'}^{m*}(\theta', \phi') O_{\ell'\ell''}^* O_{\ell\ell''}}{\omega_- \left(e^{-\frac{\omega_-}{T}} - 1 \right)} \right] \end{aligned} \quad (\text{A33})$$

and

$$\begin{aligned}
i\epsilon\mu(\partial'_t - \partial_t)\langle: \hat{\Phi}^{\text{scat}\dagger}(\mathbf{x})\hat{\Phi}^{\text{scat}}(\mathbf{x}') : \rangle &= \int dk \frac{(\omega_+ + \epsilon\mu)^2 k^2}{\pi |\omega_+ \omega_-|} \sum_{\ell, \ell', m} \sum_{\ell''=|m|} |w_{\ell''}(r_0)|^2 \times \\
&\times \left[2\epsilon\mu\omega_+ e^{i\omega_+(t-t')} \frac{v_\ell^*(r)v_{\ell'}(r')}{v_\ell^*(r_0)v_{\ell'}(r_0)} \frac{Y_\ell^{m*}(\theta, \phi)Y_{\ell'}^m(\theta', \phi')O_{\ell\ell''}^*O_{\ell'\ell''}}{\omega_+ \left(e^{\frac{\omega_+}{T}} - 1\right)} \right. \\
&\left. - 2\epsilon\mu\omega_- e^{i\omega_-(t-t')} \frac{v_\ell(r)v_{\ell'}^*(r')}{v_\ell(r_0)v_{\ell'}^*(r_0)} \frac{Y_\ell^m(\theta, \phi)Y_{\ell'}^{m*}(\theta', \phi')O_{\ell\ell''}^*O_{\ell'\ell''}}{\omega_- \left(e^{-\frac{\omega_-}{T}} - 1\right)} \right] \quad (\text{A34})
\end{aligned}$$

Putting these terms together and using the dispersion relation (10), we can write for the energy-momentum tensor:

$$T_{rr}^{\text{scat}/\text{scat}} = \frac{1}{2} (k^2 + \partial_r \partial'_r) \langle: \hat{\Phi}^{\text{scat}\dagger}(\mathbf{x})\hat{\Phi}^{\text{scat}}(\mathbf{x}') : \rangle |_{\mathbf{x}'=\mathbf{x}} \quad (\text{A35})$$

Now all that remains to be done are the radial derivatives. Since the function $v_\ell(r)$ satisfies the boundary condition at infinity (discussed in sec III B) given by:

$$v_\ell(r) \simeq e^{-i\frac{\pi}{2}(\ell+1)} \frac{e^{i(kr-\eta \ln 2kr)}}{kr} \quad (\text{A36})$$

and whose derivative at leading order is:

$$\partial_r v_\ell(r) \simeq i e^{-i\frac{\pi}{2}(\ell+1)} \frac{e^{i(kr-\eta \ln 2kr)}}{r} = ikv_\ell(r) \quad (\text{A37})$$

Then, at leading order in this limit, we have for the component $T_{rr}^{\text{scat}/\text{scat}}$:

$$T_{rr}^{\text{scat}/\text{scat}} = k^2 \langle: \hat{\Phi}^{\text{scat}\dagger}(\mathbf{x})\hat{\Phi}^{\text{scat}}(\mathbf{x}') : \rangle |_{\mathbf{x}'=\mathbf{x}} \quad (\text{A38})$$

Now, replacing with (A25), using the asymptotic limit (A36) of $v_\ell(r)$ and taking $\mathbf{x}' = \mathbf{x}$, we obtain:

$$\begin{aligned}
T_{rr}^{\text{scat}/\text{scat}} &= \int_0^\infty dk \frac{(\omega_+ + \epsilon\mu)^2 k^2}{\pi |\omega_+ \omega_-|} \sum_{\ell, \ell', m} \sum_{\ell''=|m|} \frac{|w_{\ell''}(r_0)|^2}{r^2} \times \\
&\left[\frac{e^{i\frac{\pi}{2}(\ell-\ell')} O_{\ell\ell''}^* O_{\ell'\ell''}}{\omega_+ \left(e^{\frac{\omega_+}{T}} - 1\right)} \frac{Y_\ell^{m*}(\theta, \phi)Y_{\ell'}^m(\theta, \phi)}{v_\ell^*(r_0)v_{\ell'}(r_0)} - \frac{e^{-i\frac{\pi}{2}(\ell-\ell')} O_{\ell\ell''}^* O_{\ell'\ell''}}{\omega_- \left(e^{-\frac{\omega_-}{T}} - 1\right)} \frac{Y_\ell^m(\theta, \phi)Y_{\ell'}^{m*}(\theta, \phi)}{v_\ell(r_0)v_{\ell'}^*(r_0)} \right] \quad (\text{A39})
\end{aligned}$$

Moreover, noting that it can be exchanged $\ell \leftrightarrow \ell'$ since it is summing over all possible values

of ℓ and ℓ' , then we finally have:

$$T_{rr}^{\text{scat/scat}} = \int_0^\infty dk \frac{(\omega_+ + \mathbf{e}\mu)^2 k^2}{\pi |\omega_+ \omega_-|} \sum_{\ell, \ell', m} \sum_{\ell''=|m|} \frac{|w_{\ell''}(r_0)|^2}{r^2} e^{i\frac{\pi}{2}(\ell-\ell')} O_{\ell\ell''}^* O_{\ell'\ell''} \frac{Y_\ell^{m*}(\theta, \phi) Y_{\ell'}^m(\theta, \phi)}{v_\ell^*(r_0) v_{\ell'}(r_0)} \times \left[\frac{1}{\omega_+ \left(e^{\frac{\omega_+}{T}} - 1 \right)} - \frac{1}{\omega_- \left(e^{-\frac{\omega_-}{T}} - 1 \right)} \right] \quad (\text{A40})$$

We compute now the component $T_{rr}^{\text{scat/inc}}$ in the same way by using the definition of T_{rr} in (A6) and the expectation value obtained in (A27). First, notice that the time dependence is the same than in the previous case with *scat/scat* fields (since the difference between the fields are in the radial functions), then using (A35) we have:

$$\begin{aligned} T_{rr}^{\text{scat/inc}} &= \frac{1}{2} (k^2 + \partial_r \partial'_r) \langle : \hat{\Phi}^{\text{scat}\dagger}(\mathbf{x}) \hat{\Phi}^{\text{inc}}(\mathbf{x}') : \rangle |_{\mathbf{x}'=\mathbf{x}} \\ &= \int dk \frac{(\omega_+ + \mathbf{e}\mu)^2 k^2}{2\pi |\omega_+ \omega_-|} \sum_{\ell, m, \ell'} |w_{\ell'}(r_0)|^2 \times \\ &\quad \times \left[(k^2 + \partial_r \partial'_r) e^{i\omega_+(t-t')} \frac{v_\ell^*(r) w_{\ell'}(r')}{v_\ell^*(r_0) w_{\ell'}(r_0)} \frac{Y_\ell^{m*}(\theta, \phi) Y_{\ell'}^m(\theta', \phi') O_{\ell\ell'}^*}{\omega_+ \left(e^{\frac{\omega_+}{T}} - 1 \right)} \right. \\ &\quad \left. - (k^2 + \partial_r \partial'_r) e^{i\omega_-(t-t')} \frac{v_\ell(r) w_{\ell'}^*(r')}{v_\ell(r_0) w_{\ell'}^*(r_0)} \frac{Y_\ell^m(\theta, \phi) Y_{\ell'}^{m*}(\theta', \phi') O_{\ell\ell'}}{\omega_- \left(e^{-\frac{\omega_-}{T}} - 1 \right)} \right]_{\mathbf{x}'=\mathbf{x}} \end{aligned} \quad (\text{A41})$$

Again, to compute the radial derivatives we use the asymptotic of $v_\ell(r)$ (A36) but we also need the asymptotic behaviour of $w_\ell(r)$ (also discussed in sec III B):

$$w_\ell(r) \simeq i \frac{e^{-i(kr - \eta \ln 2kr + \frac{\ell\pi}{2})}}{2kr} \left((-1)^\ell - e^{i2(kr - \eta \ln 2kr)} \right) \quad (\text{A42})$$

and whose derivative at leader order is:

$$\partial_r w_\ell(r) \simeq \frac{e^{-i(kr - \eta \ln 2kr + \frac{\ell\pi}{2})} \left((-1)^\ell + e^{i2(kr - \eta \ln 2kr)} \right)}{2r} \quad (\text{A43})$$

Then, replacing in $T_{rr}^{\text{scat/inc}}$ with this asymptotic functions behavior and taking $\mathbf{x}' = \mathbf{x}$ we have:

$$T_{rr}^{\text{scat/inc}} = \int dk \frac{(\omega_+ + \mathbf{e}\mu)^2 k^2}{\pi |\omega_+ \omega_-|} \sum_{\ell, m, \ell'} \frac{|w_{\ell'}(r_0)|^2}{2r^2} \left[\frac{e^{i\frac{\pi}{2}(\ell-\ell')}}{v_\ell^*(r_0) w_{\ell'}(r_0)} \frac{Y_\ell^{m*}(\theta, \phi) Y_{\ell'}^m(\theta, \phi) O_{\ell\ell'}^*}{\omega_+ \left(e^{\frac{\omega_+}{T}} - 1 \right)} - \frac{e^{-i\frac{\pi}{2}(\ell-\ell')}}{v_\ell(r_0) w_{\ell'}^*(r_0)} \frac{Y_\ell^m(\theta, \phi) Y_{\ell'}^{m*}(\theta, \phi) O_{\ell\ell'}}{\omega_- \left(e^{-\frac{\omega_-}{T}} - 1 \right)} \right] \quad (\text{A44})$$

Since ℓ and ℓ' are dummy indices, we can simplify a bit by interchanging $\ell \leftrightarrow \ell'$ in the second line, finally getting:

$$T_{rr}^{\text{scat/inc}} = \int dk \frac{(\omega_+ + \mathbf{e}\mu)^2 k^2}{\pi |\omega_+ \omega_-| 2r^2} \sum_{\ell, m, \ell'} e^{i\frac{\pi}{2}(\ell - \ell')} Y_\ell^{m*}(\theta, \phi) Y_{\ell'}^m(\theta, \phi) \times \left[\frac{w_{\ell'}^*(r_0)}{v_{\ell'}^*(r_0)} \frac{O_{\ell'\ell}^*}{\omega_+ \left(e^{\frac{\omega_+}{T}} - 1 \right)} - \frac{w_\ell(r_0)}{v_\ell(r_0)} \frac{O_{\ell\ell}}{\omega_- \left(e^{-\frac{\omega_-}{T}} - 1 \right)} \right] \quad (\text{A45})$$

We compute now the component $T_{rr}^{\text{inc/scat}}$ in the same way by using the definition of T_{rr} in (A6) and the expectation value obtained in (A29). Again, the time dependence is the same as in the other cases. Then, using (A35) we have:

$$T_{rr}^{\text{inc/scat}} = \frac{1}{2} (k^2 + \partial_r \partial_r') \langle : \hat{\Phi}^{\text{inc}\dagger}(\mathbf{x}) \hat{\Phi}^{\text{scat}}(\mathbf{x}') : \rangle |_{\mathbf{x}'=\mathbf{x}} = \int dk \frac{(\omega_+ + \mathbf{e}\mu)^2 k^2}{2\pi |\omega_+ \omega_-|} \sum_{\ell, m, \ell'} |w_\ell(r_0)|^2 \times \left[(k^2 + \partial_r \partial_r') e^{i\omega_+(t-t')} \frac{w_\ell^*(r) v_{\ell'}(r')}{w_\ell^*(r_0) v_{\ell'}(r_0)} \frac{Y_\ell^{m*}(\theta, \phi) Y_{\ell'}^m(\theta', \phi') O_{\ell'\ell}}{\omega_+ \left(e^{\frac{\omega_+}{T}} - 1 \right)} - (k^2 + \partial_r \partial_r') e^{i\omega_-(t-t')} \frac{w_\ell(r) v_{\ell'}^*(r')}{w_\ell(r_0) v_{\ell'}^*(r_0)} \frac{Y_\ell^m(\theta, \phi) Y_{\ell'}^{m*}(\theta', \phi') O_{\ell'\ell}^*}{\omega_- \left(e^{-\frac{\omega_-}{T}} - 1 \right)} \right]_{\mathbf{x}'=\mathbf{x}} \quad (\text{A46})$$

Replacing with the asymptotic functions behavior and taking $\mathbf{x}' = \mathbf{x}$ we have:

$$T_{rr}^{\text{inc/scat}} = \int dk \frac{(\omega_+ + \mathbf{e}\mu)^2 k^2}{\pi |\omega_+ \omega_-|} \sum_{\ell, m, \ell'} \frac{|w_\ell(r_0)|^2}{2r^2} \left[\frac{e^{-i\frac{\pi}{2}(\ell' - \ell)} Y_\ell^{m*}(\theta, \phi) Y_{\ell'}^m(\theta, \phi) O_{\ell'\ell}}{w_\ell^*(r_0) v_{\ell'}(r_0) \omega_+ \left(e^{\frac{\omega_+}{T}} - 1 \right)} - \frac{e^{i\frac{\pi}{2}(\ell' - \ell)} Y_\ell^m(\theta, \phi) Y_{\ell'}^{m*}(\theta, \phi) O_{\ell'\ell}^*}{w_\ell(r_0) v_{\ell'}^*(r_0) \omega_- \left(e^{-\frac{\omega_-}{T}} - 1 \right)} \right] \quad (\text{A47})$$

Since ℓ and ℓ' are dummy indices, we can simplify a bit by interchanging $\ell \leftrightarrow \ell'$ in the first line, finally getting:

$$T_{rr}^{\text{inc/scat}} = \int dk \frac{(\omega_+ + \mathbf{e}\mu)^2 k^2}{\pi |\omega_+ \omega_-| 2r^2} \sum_{\ell, m, \ell'} e^{-i\frac{\pi}{2}(\ell - \ell')} Y_\ell^m(\theta, \phi) Y_{\ell'}^{m*}(\theta, \phi) \times \left[\frac{w_{\ell'}(r_0)}{v_{\ell'}(r_0)} \frac{O_{\ell\ell'}}{\omega_+ \left(e^{\frac{\omega_+}{T}} - 1 \right)} - \frac{w_\ell^*(r_0)}{v_\ell^*(r_0)} \frac{O_{\ell'\ell}^*}{\omega_- \left(e^{-\frac{\omega_-}{T}} - 1 \right)} \right] \quad (\text{A48})$$

Note that comparing with the component $T_{rr}^{\text{scat/inc}}$ in (A45) we have:

$$T_{rr}^{\text{inc/scat}} = (T_{rr}^{\text{scat/inc}})^* \quad (\text{A49})$$

Lastly, bringing together the three calculated terms in T_{rr} (expressions A40, A45 and A49) and multiplying by r^2 (as appears in the total thrust force in sec IV B) we obtain:

$$\begin{aligned}
r^2 T_{rr} &= r^2 T_{rr}^{\text{scat}/\text{scat}} + 2r^2 \Re [T_{rr}^{\text{scat}/\text{inc}}] \\
&= \int_0^\infty dk \frac{(\omega_+ + \mathbf{e}\mu)^2 k^2}{\pi |\omega_+ \omega_-|} \sum_{\ell, \ell', m} \left\{ \sum_{\ell''=|m|} |w_{\ell''}(r_0)|^2 e^{i\frac{\pi}{2}(\ell-\ell')} \frac{Y_\ell^{m*}(\theta, \phi) Y_{\ell'}^m(\theta, \phi)}{v_\ell^*(r_0) v_{\ell'}(r_0)} \times \right. \\
&\quad \times O_{\ell\ell''}^{m*} O_{\ell'\ell''}^m \left(\frac{1}{\omega_+ \left(e^{\frac{\omega_+}{T}} - 1 \right)} - \frac{1}{\omega_- \left(e^{-\frac{\omega_-}{T}} - 1 \right)} \right) \\
&\quad \left. + 2 \Re \left[\frac{1}{2} e^{i\frac{\pi}{2}(\ell-\ell')} Y_\ell^{m*}(\theta, \phi) Y_{\ell'}^m(\theta, \phi) \frac{w_{\ell'}^*(r_0)}{v_\ell^*(r_0)} \frac{O_{\ell\ell'}^{m*}}{\omega_+ \left(e^{\frac{\omega_+}{T}} - 1 \right)} \right. \right. \\
&\quad \left. \left. - \frac{1}{2} e^{i\frac{\pi}{2}(\ell-\ell')} Y_\ell^{m*}(\theta, \phi) Y_{\ell'}^m(\theta, \phi) \frac{w_\ell(r_0)}{v_{\ell'}(r_0)} \frac{O_{\ell'\ell}^m}{\omega_- \left(e^{-\frac{\omega_-}{T}} - 1 \right)} \right] \right\} \quad (\text{A50})
\end{aligned}$$

If we now interchange $\ell \leftrightarrow \ell'$ in the last line, replace with the conjugate and regrouping the remaining terms, we can finally write:

$$\begin{aligned}
r^2 T_{rr} &= \int_0^\infty dk \frac{(\omega_+ + \mathbf{e}\mu)^2 k^2}{\pi |\omega_+ \omega_-|} \left(\frac{1}{\omega_+ \left(e^{\frac{\omega_+}{T}} - 1 \right)} - \frac{1}{\omega_- \left(e^{-\frac{\omega_-}{T}} - 1 \right)} \right) \times \\
&\quad \times \sum_{\ell, \ell', m} \mathcal{U}_{\ell\ell'} Y_\ell^{m*}(\theta, \phi) Y_{\ell'}^m(\theta, \phi) \quad (\text{A51})
\end{aligned}$$

where we defined

$$\mathcal{U}_{\ell\ell'}^m = \sum_{\ell''=|m|} e^{i\frac{\pi}{2}(\ell-\ell')} \frac{|w_{\ell''}(r_0)|^2}{v_\ell^*(r_0) v_{\ell'}(r_0)} O_{\ell\ell''}^{m*} O_{\ell'\ell''}^m + \Re \left[e^{i\frac{\pi}{2}(\ell-\ell')} \frac{w_\ell(r_0)}{v_{\ell'}(r_0)} O_{\ell'\ell}^m \right] \quad (\text{A52})$$

4. Computation of $T_{r\theta}$

We now compute the other energy-momentum tensor component of interest for calculating the thrust force in sec IV B, $rT_{r\theta}$. We use its definition (A7):

$$T_{r\theta} = \frac{1}{2} (\partial_r \partial'_\theta + \partial'_r \partial_\theta) \langle : \hat{\Phi}^\dagger(\mathbf{x}) \hat{\Phi}(\mathbf{x}') : \rangle |_{\mathbf{x}'=\mathbf{x}} \quad (\text{A53})$$

and we calculate this component using each expectation value of the field obtained in sec A 2. Beginning with the component $T_{r\theta}^{\text{scat}/\text{scat}}$, we use (A25):

$$\begin{aligned}
rT_{r\theta}^{\text{scat}/\text{scat}} &= \frac{1}{2}r (\partial_r \partial_{\theta'} + \partial_{r'} \partial_{\theta}) \langle : \hat{\Phi}^{\text{scat}\dagger}(\mathbf{x}) \hat{\Phi}^{\text{scat}}(\mathbf{x}') : \rangle |_{\mathbf{x}'=\mathbf{x}} \\
&= \int dk \frac{(\omega_+ + \mathbf{e}\mu)^2 k^2 r}{2\pi |\omega_+ \omega_-|} \sum_{\ell, \ell', m} \sum_{\ell''=|m|} |w_{\ell''}(r_0)|^2 \times \\
&\quad \times \left[e^{i\omega_+(t-t')} \frac{\partial_r v_{\ell}^*(r) v_{\ell'}(r')}{v_{\ell}^*(r_0) v_{\ell'}(r_0)} \frac{Y_{\ell}^{m*}(\theta, \phi) \partial_{\theta'} Y_{\ell'}^m(\theta', \phi) O_{\ell\ell''}^* O_{\ell'\ell''}}{\omega_+ \left(e^{\frac{\omega_+}{T}} - 1 \right)} \right. \\
&\quad - e^{i\omega_-(t-t')} \frac{\partial_r v_{\ell}(r) v_{\ell'}^*(r')}{v_{\ell}(r_0) v_{\ell'}^*(r_0)} \frac{Y_{\ell}^m(\theta, \phi) \partial_{\theta'} Y_{\ell'}^{m*}(\theta', \phi) O_{\ell\ell''}^* O_{\ell'\ell''}}{\omega_- \left(e^{-\frac{\omega_-}{T}} - 1 \right)} \\
&\quad + e^{i\omega_+(t-t')} \frac{v_{\ell}^*(r) \partial_r v_{\ell'}(r')}{v_{\ell}^*(r_0) v_{\ell'}(r_0)} \frac{\partial_{\theta} Y_{\ell}^{m*}(\theta, \phi) Y_{\ell'}^m(\theta', \phi) O_{\ell\ell''}^* O_{\ell'\ell''}}{\omega_+ \left(e^{\frac{\omega_+}{T}} - 1 \right)} \\
&\quad \left. - e^{i\omega_-(t-t')} \frac{v_{\ell}(r) \partial_r v_{\ell'}^*(r')}{v_{\ell}(r_0) v_{\ell'}^*(r_0)} \frac{\partial_{\theta} Y_{\ell}^m(\theta, \phi) Y_{\ell'}^{m*}(\theta', \phi) O_{\ell\ell''}^* O_{\ell'\ell''}}{\omega_- \left(e^{-\frac{\omega_-}{T}} - 1 \right)} \right]_{\mathbf{x}'=\mathbf{x}} \tag{A54}
\end{aligned}$$

Using the asymptotic form of $v_{\ell}(r)$ in (A36) and taking $\mathbf{x}' = \mathbf{x}$ we have:

$$\begin{aligned}
rT_{r\theta}^{\text{scat}/\text{scat}} &= \int dk \frac{(\omega_+ + \mathbf{e}\mu)^2 ik}{2\pi |\omega_+ \omega_-|} \frac{1}{r} \sum_{\ell, \ell', m} \sum_{\ell''=|m|} |w_{\ell''}(r_0)|^2 \times \\
&\quad \times \left[e^{i\frac{\pi}{2}(\ell-\ell')} \frac{O_{\ell\ell''}^* O_{\ell'\ell''}}{v_{\ell}^*(r_0) v_{\ell'}(r_0)} \left(\frac{Y_{\ell'}^m(\theta, \phi) \partial_{\theta} Y_{\ell}^{m*}(\theta, \phi) - Y_{\ell}^{m*}(\theta, \phi) \partial_{\theta} Y_{\ell'}^m(\theta, \phi)}{\omega_+ \left(e^{\frac{\omega_+}{T}} - 1 \right)} \right) \right. \\
&\quad \left. - e^{-i\frac{\pi}{2}(\ell-\ell')} \frac{O_{\ell'\ell''}^* O_{\ell\ell''}}{v_{\ell}(r_0) v_{\ell'}^*(r_0)} \left(\frac{Y_{\ell}^m(\theta, \phi) \partial_{\theta} Y_{\ell'}^{m*}(\theta, \phi) - Y_{\ell'}^{m*}(\theta, \phi) \partial_{\theta} Y_{\ell}^m(\theta, \phi)}{\omega_- \left(e^{-\frac{\omega_-}{T}} - 1 \right)} \right) \right] \tag{A55}
\end{aligned}$$

Note that this component is $\mathcal{O}(r^{-1})$.

We obtain in the same way the component $rT_{r\theta}^{\text{scat/inc}}$ by using (A27):

$$\begin{aligned}
rT_{r\theta}^{\text{scat/inc}} &= \frac{1}{2} r (\partial_r \partial'_\theta + \partial'_r \partial_\theta) \langle : \hat{\Phi}^{\text{scat}\dagger}(\mathbf{x}) \hat{\Phi}^{\text{inc}}(\mathbf{x}') : \rangle |_{\mathbf{x}'=\mathbf{x}} \\
&= \int dk \frac{(\omega_+ + \mathbf{e}\mu)^2 k^2 r}{2\pi |\omega_+ \omega_-|} \sum_{\ell, m, \ell'} |w_{\ell'}(r_0)|^2 \times \\
&\quad \times \left[\begin{aligned}
&e^{i\omega_+(t-t')} \frac{\partial_r v_\ell^*(r) w_{\ell'}(r')}{v_\ell^*(r_0) w_{\ell'}(r_0)} \frac{Y_\ell^{m*}(\theta, \phi) \partial'_\theta Y_{\ell'}^m(\theta', \phi') O_{\ell\ell'}^*}{\omega_+ \left(e^{\frac{\omega_+}{T}} - 1 \right)} \\
&+ e^{i\omega_+(t-t')} \frac{v_\ell^*(r) \partial'_r w_{\ell'}(r')}{v_\ell^*(r_0) w_{\ell'}(r_0)} \frac{\partial_\theta Y_\ell^{m*}(\theta, \phi) Y_{\ell'}^m(\theta', \phi') O_{\ell\ell'}^*}{\omega_+ \left(e^{\frac{\omega_+}{T}} - 1 \right)} \\
&- e^{i\omega_-(t-t')} \frac{\partial_r v_\ell(r) w_{\ell'}^*(r')}{v_\ell(R) w_{\ell'}^*(r_0)} \frac{Y_\ell^m(\theta, \phi) \partial'_\theta Y_{\ell'}^{m*}(\theta', \phi') O_{\ell\ell'}}{\omega_- \left(e^{-\frac{\omega_-}{T}} - 1 \right)} \\
&- e^{i\omega_-(t-t')} \frac{v_\ell(r) \partial'_r w_{\ell'}^*(r')}{v_\ell(r_0) w_{\ell'}^*(r_0)} \frac{\partial_\theta Y_\ell^m(\theta, \phi) Y_{\ell'}^{m*}(\theta', \phi') O_{\ell\ell'}}{\omega_- \left(e^{-\frac{\omega_-}{T}} - 1 \right)} \end{aligned} \right]_{\mathbf{x}'=\mathbf{x}} \tag{A56}
\end{aligned}$$

Using the asymptotic form of $v_\ell(r)$ and $w_\ell(r)$ in (A36) and (A42) respectively, and taking $\mathbf{x}' = \mathbf{x}$ we have:

$$\begin{aligned}
rT_{r\theta}^{\text{scat/inc}} &= \int dk \frac{(\omega_+ + \mathbf{e}\mu)^2 k^2 r}{4\pi |\omega_+ \omega_-|} \frac{k}{r} \sum_{\ell, m, \ell'} |w_{\ell'}(r_0)|^2 \times \\
&\quad \times \left[\begin{aligned}
&\frac{e^{i\frac{\pi}{2}(\ell-\ell'+1)} \left((-1)^{\ell'} e^{-i2kr} - 1 \right) Y_\ell^{m*}(\theta, \phi) \partial_\theta Y_{\ell'}^m(\theta, \phi) O_{\ell\ell'}^*}{v_\ell^*(r_0) w_{\ell'}(r_0) \omega_+ \left(e^{\frac{\omega_+}{T}} - 1 \right)} \\
&+ \frac{e^{i\frac{\pi}{2}(\ell-\ell'+1)} \left((-1)^{\ell'} e^{-i2kr} + 1 \right) \partial_\theta Y_\ell^{m*}(\theta, \phi) Y_{\ell'}^m(\theta, \phi) O_{\ell\ell'}^*}{v_\ell^*(r_0) w_{\ell'}(r_0) \omega_+ \left(e^{\frac{\omega_+}{T}} - 1 \right)} \\
&- \frac{e^{-i\frac{\pi}{2}(\ell-\ell'+1)} \left((-1)^{\ell'} e^{i2kr} - 1 \right) Y_\ell^m(\theta, \phi) \partial_\theta Y_{\ell'}^{m*}(\theta, \phi) O_{\ell\ell'}}{v_\ell(r_0) w_{\ell'}^*(r_0) \omega_- \left(e^{-\frac{\omega_-}{T}} - 1 \right)} \\
&- \frac{e^{-i\frac{\pi}{2}(\ell-\ell'+1)} \left((-1)^{\ell'} e^{i2kr} + 1 \right) \partial_\theta Y_\ell^m(\theta, \phi) Y_{\ell'}^{m*}(\theta, \phi) O_{\ell\ell'}}{v_\ell(r_0) w_{\ell'}^*(r_0) \omega_- \left(e^{-\frac{\omega_-}{T}} - 1 \right)} \end{aligned} \right] \tag{A57}
\end{aligned}$$

Also, note that this component is $\mathcal{O}(r^{-1})$.

Finally we obtain the component $T_{r\theta}^{\text{inc/scat}}$ by using (A29):

$$\begin{aligned}
rT_{r\theta}^{\text{inc/scat}} &= \frac{1}{2}r (\partial_r \partial'_\theta + \partial'_r \partial_\theta) \langle : \hat{\Phi}^{\text{inc}\dagger}(\mathbf{x}) \hat{\Phi}^{\text{scat}}(\mathbf{x}') : \rangle |_{\mathbf{x}'=\mathbf{x}} \\
&= \int dk \frac{(\omega_+ + \mathbf{e}\mu)^2 k^2 r}{2\pi |\omega_+ \omega_-|} \sum_{\ell, m, \ell'} |w_\ell(r_0)|^2 \times \\
&\quad \times \left[e^{i\omega_+(t-t')} \frac{\partial_r w_\ell^*(r) v_{\ell'}(r')}{w_\ell^*(r_0) v_{\ell'}(r_0)} \frac{Y_\ell^{m*}(\theta, \phi) \partial'_\theta Y_{\ell'}^m(\theta', \phi) O_{\ell'\ell}}{\omega_+ \left(e^{\frac{\omega_+}{T}} - 1 \right)} \right. \\
&\quad + e^{i\omega_+(t-t')} \frac{w_\ell^*(r) \partial'_r v_{\ell'}(r')}{w_\ell^*(r_0) v_{\ell'}(r_0)} \frac{\partial_\theta Y_\ell^{m*}(\theta, \phi) Y_{\ell'}^m(\theta', \phi) O_{\ell'\ell}}{\omega_+ \left(e^{\frac{\omega_+}{T}} - 1 \right)} \\
&\quad - e^{-i\omega_+(t-t')} \frac{\partial_r w_\ell(r) v_{\ell'}^*(r')}{w_\ell(r_0) v_{\ell'}^*(r_0)} \frac{Y_\ell^m(\theta, \phi) \partial'_\theta Y_{\ell'}^{m*}(\theta', \phi) O_{\ell'\ell}^*}{\omega_- \left(e^{-\frac{\omega_-}{T}} - 1 \right)} \\
&\quad \left. - e^{-i\omega_+(t-t')} \frac{w_\ell(r) \partial'_r v_{\ell'}^*(r')}{w_\ell(r_0) v_{\ell'}^*(r_0)} \frac{\partial_\theta Y_\ell^m(\theta, \phi) Y_{\ell'}^{m*}(\theta', \phi) O_{\ell'\ell}^*}{\omega_- \left(e^{-\frac{\omega_-}{T}} - 1 \right)} \right]_{\mathbf{x}'=\mathbf{x}} \tag{A58}
\end{aligned}$$

Using the asymptotic form of $v_\ell(r)$ and $w_\ell(r)$ in (A36) and (A42) respectively, and taking $\mathbf{x}' = \mathbf{x}$ we have:

$$\begin{aligned}
rT_{r\theta}^{\text{inc/scat}} &= \int dk \frac{(\omega_+ + \mathbf{e}\mu)^2 k}{4\pi |\omega_+ \omega_-|} \frac{1}{r} \sum_{\ell, m, \ell'} |w_\ell(r_0)|^2 \times \\
&\quad \times \left[e^{-i\frac{\pi}{2}(\ell'-\ell+1)} \frac{((-1)^\ell e^{i2kr} + 1)}{w_\ell^*(r_0) v_{\ell'}(r_0)} \frac{Y_\ell^{m*}(\theta, \phi) \partial_\theta Y_{\ell'}^m(\theta, \phi) O_{\ell'\ell}}{\omega_+ \left(e^{\frac{\omega_+}{T}} - 1 \right)} \right. \\
&\quad + e^{-i\frac{\pi}{2}(\ell'-\ell+1)} \frac{((-1)^\ell e^{i2kr} - 1)}{w_\ell^*(r_0) v_{\ell'}(r_0)} \frac{\partial_\theta Y_\ell^{m*}(\theta, \phi) Y_{\ell'}^m(\theta, \phi) O_{\ell'\ell}}{\omega_+ \left(e^{\frac{\omega_+}{T}} - 1 \right)} \\
&\quad - e^{i\frac{\pi}{2}(\ell'-\ell+1)} \frac{((-1)^\ell e^{-2ikr} + 1)}{w_\ell(r_0) v_{\ell'}^*(r_0)} \frac{Y_\ell^m(\theta, \phi) \partial_\theta Y_{\ell'}^{m*}(\theta, \phi) O_{\ell'\ell}^*}{\omega_- \left(e^{-\frac{\omega_-}{T}} - 1 \right)} \\
&\quad \left. - e^{i\frac{\pi}{2}(\ell'-\ell+1)} \frac{((-1)^\ell e^{-2ikr} - 1)}{w_\ell(r_0) v_{\ell'}^*(r_0)} \frac{\partial_\theta Y_\ell^m(\theta, \phi) Y_{\ell'}^{m*}(\theta, \phi) O_{\ell'\ell}^*}{\omega_- \left(e^{-\frac{\omega_-}{T}} - 1 \right)} \right] \tag{A59}
\end{aligned}$$

Again, note that this component is $\mathcal{O}(r^{-1})$.

In conclusion, bringing together the three components of $T_{r\theta}$ we see that this component is $\mathcal{O}(r^{-1})$. On the other hand, the other term in the force is $r^2 T_{rr}$ (which we already computed in sec A 3) and it is $\mathcal{O}(r^0)$. Therefore, at leading order when $r \rightarrow \infty$, the component $rT_{r\theta}$ vanishes.

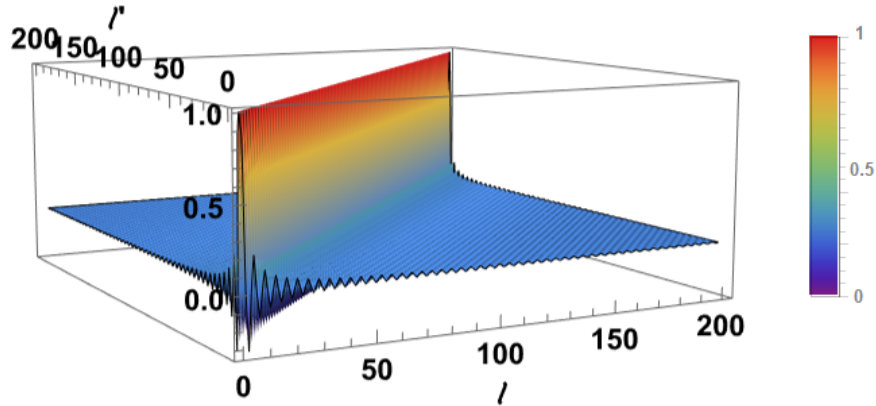


FIG. 10: Matrix of coefficients $\gamma_{\ell\ell'}^m$ with $m = 0$.

Appendix B: Numerical Complement

1. γ^m Analysis

The results obtained in sections III D and IV C depend on m matrices of coefficients $\gamma_{\ell\ell'}^m$ (defined in (26)) and which do not depend on the system parameters. As can be seen in fig 10, these matrices have their highest value on the diagonal $\gamma_{\ell\ell}^m = 1$ and oscillate around zero as we move away from the diagonal. This behaviour will allow us to cut down the matrix and still grasp the physics of it.

2. Numerical Cutoff

In order to obtain the numerical results we need to define a cutoff in the sums over ℓ (cutting ℓ we have cut the sum over m as well since $\ell > |m|$). To do so, first we notice that the result for the matching in sec III C depends on the radial functions evaluated at the mirror. Moreover, the result depends indirectly on the inverse of the derivative¹ $R_\ell'(r_m)$ (these are inside the definition of H_ℓ which is inside of M^m defined in (28); for our results we need the inverse $(M^m)^{-1}$). Then, analyzing the radial equation (5):

$$\frac{1}{r^2} \partial_r (r^2 f(r) \partial_r R_\ell(r)) + \left(\frac{(\omega + e h(r))^2}{f(r)} - \frac{\ell(\ell + 1)}{r^2} - m^2 \right) R_\ell(r) = 0 \quad (\text{B1})$$

¹ Here we use the notation $R_\ell(r)$ to refer to all the radial solutions $u_\ell(r)$, $v_\ell(r)$ and $w_\ell(r)$.

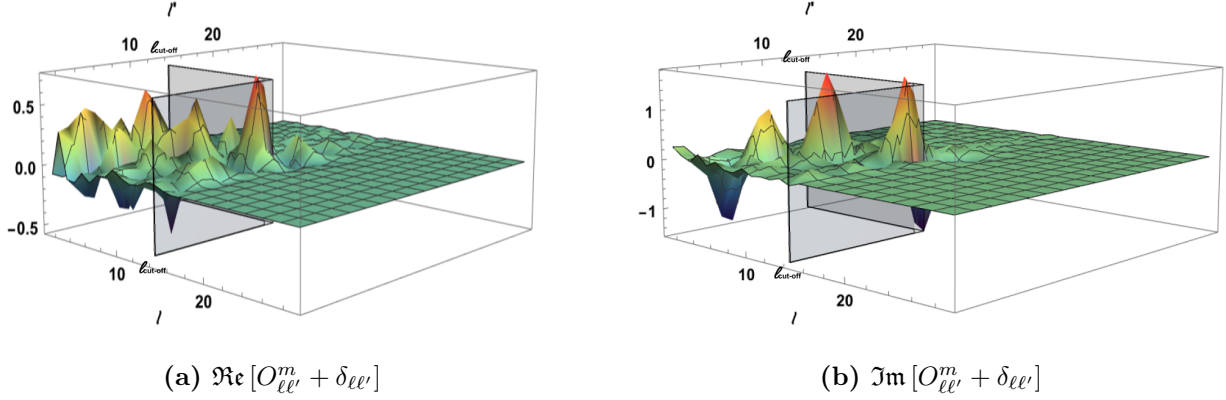


FIG. 11: Elements of $O_{\ell\ell'}^m + \delta_{\ell\ell'}$ with $m = 0$ and $k = 0.3$, we mark the value $\ell_{\text{cutoff}} = 14$ (in this case) where a peak is predicted.

If we define

$$y_\ell(r) = r^2 f(r) R'_\ell(r) \quad (\text{B2})$$

we have:

$$y'_\ell(r) = -r^2 \left(\frac{(\omega + eh(r))^2}{f(r)} - \frac{\ell(\ell + 1)}{r^2} - m^2 \right) R_\ell(r) \quad (\text{B3})$$

$$R'_\ell(r) = \frac{y_\ell(r)}{r^2 f(r)} \quad (\text{B4})$$

Note that the parenthesis $\left(\frac{(\omega + eh(r))^2}{f(r)} - \frac{\ell(\ell + 1)}{r^2} - m^2 \right)$ vanishes at a certain value of ℓ (for k and r fixed), therefore the derivative $y'_\ell(r)$ is zero and we have a minimum of $R'_\ell(r)$. Then, for this value of ℓ we have a maximum of $(R'_\ell(r))^{-1}$, so taking $r = r_m$ we define ℓ_{cutoff} as:

$$\frac{(\omega + eh(r_0))^2}{f(r_0)} - \frac{\ell_{\text{cutoff}}(\ell_{\text{cutoff}} + 1)}{r_0^2} - m^2 = 0 \quad (\text{B5})$$

which depends on the value of k . This behaviour can be seen in fig 11, where the predicted peak is near the ℓ_{cutoff} . Then, to ensure that we are having a good approximation in the numerical analysis we take $\ell_{\text{max}} = \ell_{\text{cutoff}} + 10$. From fig 11 we also see that for $\ell > \ell_{\text{max}}$ and far away from the diagonal this does not go to zero, which means that the matching will be better if we take more ℓ . However, for the thrust force (39) we only need the values near the diagonal which we see that go to zero for $\ell > \ell_{\text{max}}$. Then, this value is a good cutoff to calculate the thrust force we are interested in.

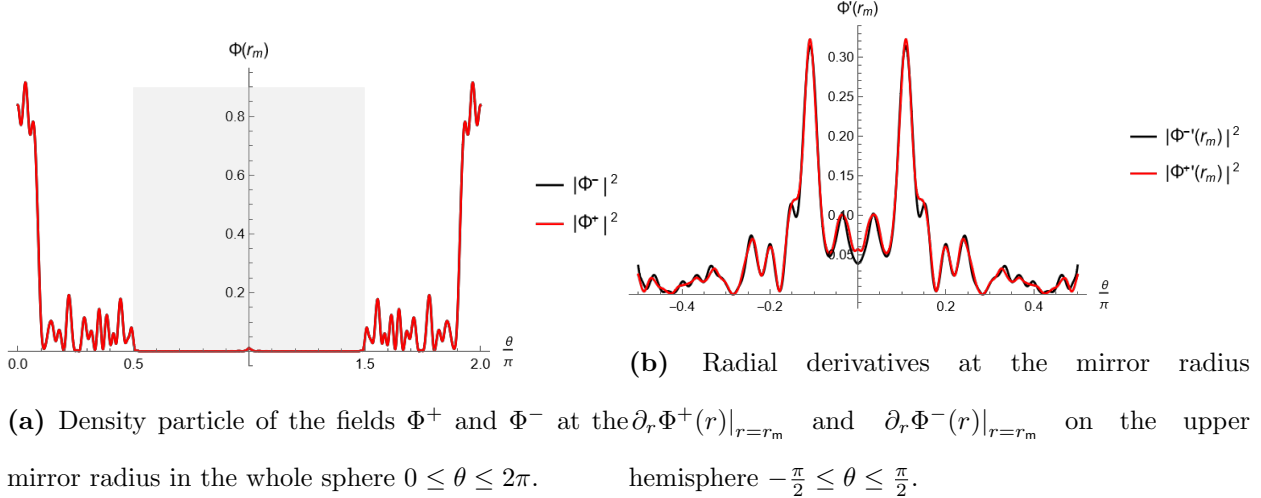


FIG. 12: Matching conditions of the obtained fields with $k = 0.6$ at the mirror radius $r = r_m = 5r_+$ and varying the angle θ . The grey region from $\frac{1}{2}\pi \leq \theta \leq \frac{3}{2}\pi$ is where the mirror is placed.

3. Matching at the Mirror

In sec IIID we show the obtained scalar field in the whole space. In fig 12 we show how this field fulfills the 3 matching conditions at the mirror radius studied in sec IIIC by using the cutoff for ℓ discussed in the previous section. First, in 12a we see the fields Φ^+ and Φ^- at $r = r_m$ where we notice that both curves coincide in the whole sphere and are zero at the mirror position, so continuity and the perfect mirror condition is satisfied. Second, in 12b we see the radial derivatives of the fields where we notice that the curves match pretty well, so continuity of the derivative (where there is no mirror) is satisfied. This matching condition can be improved by taking more values of ℓ . However, we see that the used cutoff already gives a good approximation of the analysed system.

4. Resonance on the Electromagnetic Cavity

In this section we study the case of a pure electromagnetic case where we change the black hole for a perfect conductor sphere of the same radius r_+ , maintaining the spherical mirror. To obtain the solution in this case, we consider a combination of the spherical Bessel solutions (the exact radial solutions of (5) in the case without the black hole) such that it

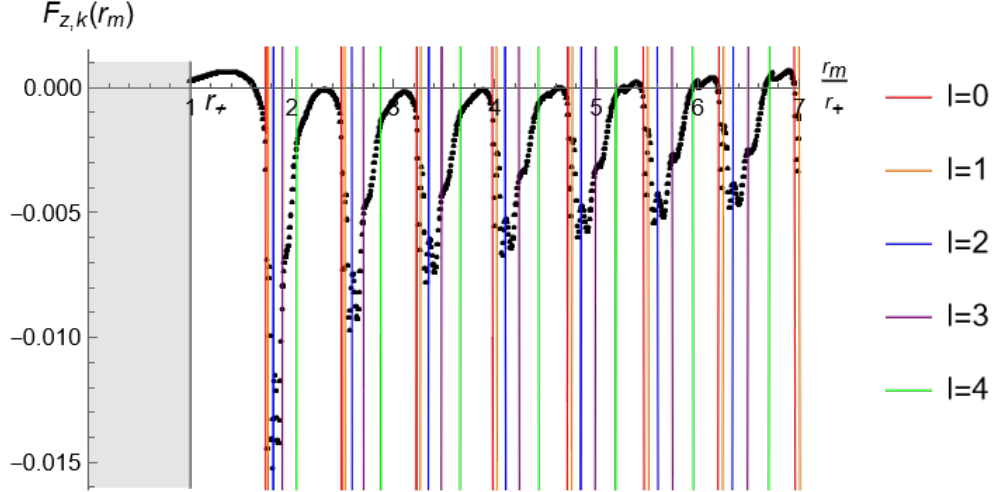


FIG. 13: Total thrust force at $k = 0.37$ obtained as function of the mirror radius r_m normalized with conductor sphere radius $r_+ = 11.4107$. Here we fix $\text{em} = 5$, $T = 0.07$, $\mu = -0.01$ and the radius r_+ correspond to a black hole horizon with $Q/M = 0.99$. The colored lines correspond to the zeros of $u_\ell(r)$ defined in (B6) and varying ℓ .

vanishes at the conductor sphere:

$$u_\ell(r) = y_\ell(kr_+)j_\ell(kr) - j_\ell(kr_+)y_\ell(kr) \quad (\text{B6})$$

In fig 13 we show the total thrust obtained for a fix value of k (this is, without performing the integral in k) in the same way than the background force in sec IV C and using the previous radial function. Moreover, we show the zeros of the function (B6) as a function of r for different ℓ . This zeros correspond for a resonant modes in the case of a closed cavity, then we see in 13 that the peaks coincide perfectly with the resonant modes where the lowest ℓ are dominant. As ℓ grows, they group together next at the right of the peaks. Therefore, we conclude that the peaks observed in sec IV C are a characteristic of the geometry and not due to the black hole, although these are modified by its presence.

-
- [1] R. Brito, V. Cardoso and P. Pani, *Superradiance*, Springer (2020) , [arXiv:1501.06570 \[gr-qc\]](#)
- [2] R. Penrose, *Gravitational collapse: The role of general relativity*, Nuovo Cimento.J. **1** (1969), 252-276
- [3] J. Bekenstein, *Extraction of energy and charge from a black hole*, Physical Review D **7.4** (1973) 949, doi: [10.1103/PhysRevD.7.949](#)
- [4] S. Carroll, *Spacetime and geometry*, Pearson Education Limited (2014)
- [5] E. Chang-Young, M. Eune, K. Kimm and D. Lee, *Surface gravity and Hawking temperature from entropic force viewpoint*, Modern Physics Letters A **25** (2010), [arXiv:1003.2049v3 \[gr-qc\]](#)
- [6] D. Gaspard, *Connection formulas between Coulomb wave functions*, Journal of Mathematical Physics **59** (2018) 112104, [arXiv:1804.10976v3 \[math-ph\]](#)
- [7] L. Acito, *Superradiant BH Rocket Open Code*, [GitHub Repository](#)
- [8] W. Greiner and J. Reinhardt, *Field quantization*, Springer (1996)
- [9] J. Kapusta, *Bose-Einstein condensation, spontaneous symmetry breaking and gauge theories*, Physical Review D **24** (1981), doi: [10.1103/PhysRevD.24.426](#)
- [10] J. Degollado, C. Herdeiro and H. Rúnarsson, *Rapid growth of superradiant instabilities for charged black holes in a cavity*, Physical Review D **88** (2013), [arXiv:1305.5513v1 \[gr-qc\]](#)
- [11] A. Arvanitaki, M. Baryakhtar, S. Dimopoulos and Sergei Dubovsky and R. Lasenby, *Black hole mergers and the QCD axion at Advanced LIGO*, Physical Review D **95** (2017), [arXiv:1604.03958v2 \[hep-ph\]](#)
- [12] V. Cardoso, O. Dias, G. Hartnett, M. Middleton, P. Pani, and J. Santos, *Constraining the mass of dark photons and axion-like particles through black-hole superradiance*, JCAP **1803** (2018) no. 03, 043, [arXiv:1801.01420 \[gr-qc\]](#)
- [13] D. Blas and S. Witte, *Imprints of axion superradiance in the CMB*, Physical Review D **102** (2020) 103018, [arXiv:2009.10074v2 \[astro-ph.CO\]](#)